Acta Oceanol. Sin., 2024, Vol. 43, No. 4, P. 61–79
https://doi.org/10.1007/s13131-024-2336-5
http://www.aosocean.com
E-mail: ocean2@hyxb.org.cn

The Middle Miocene lobe-shaped and band-shaped submarine fans in the Lingshui Sag, Qiongdongnan Basin: source-to-sink system, genesis and implication

Xingzong Yao[1, 2], Congjun Feng[1, 2*], Hongjun Qu[1, 2], Min Zhang[3], Daming Li[4]

[1] State Key Laboratory of Continental Dynamics, Northwest University, Xi'an 710069, China

[2] Department of Geology, Northwest University, Xi'an 710069, China

[3] Exploration and Development Technology Research Center of Yanchang Oilfield Co., Ltd., Yan'an 716000, China

[4] Chexplor Resource Exploration Technology Co., Ltd., Huaibei 235000, China

Received 18 December 2023; accepted 15 April 2024

Abstract

Deepwater oil and gas exploration is the key to sustainable breakthroughs in petroleum exploration worldwide. The Central Canyon gas field has confirmed the Lingshui Sag is a hydrocarbon-generating sag, and the deepwater reservoirs in the Lingshui Sag still have more fabulous oil and gas exploration potential. Based on drilling data and three-dimensional (3D) seismic data, this paper uses seismic facies analysis, seismic attribute analysis, and coherence slice analysis to identify the types of submarine fans (lobe-shaped and band-shaped submarine fans) that developed in the Lingshui Sag during the Middle Miocene, clarify the source-to-sink system of the submarine fans and discuss the genesis mechanism of the submarine fans. The results show that: (1) the deepwater source-to-sink system of the Lingshui Sag in the Middle Miocene mainly consisted of a "delta (sediment supply) - submarine canyon (sediment transport channel) - submarine fan (deepwater sediment sink)" association; (2) the main factor controlling the formation of the submarine fans developed in the Lingshui Sag was on the relative sea level decline; and (3) the bottom current reworked the lobe-shaped submarine fan that developed in the northern Lingshui Sag and formed the band-shaped submarine fan with a greater sand thickness. This paper aims to provide practical geological knowledge for subsequent petroleum exploration and development in the deepwater area of the Qiongdongnan Basin through a detailed analysis of the Middle Miocene submarine fan sedimentary system developed in the Lingshui Sag.

Key words: submarine fan, source-to-sink system, genesis mechanism, Middle Miocene, Lingshui Sag

Citation: Yao Xingzong, Feng Congjun, Qu Hongjun, Zhang Min, Li Daming. 2024. The Middle Miocene lobe-shaped and band-shaped submarine fans in the Lingshui Sag, Qiongdongnan Basin: source-to-sink system, genesis and implication. Acta Oceanologica Sinica, 43(4): 61–79, doi: 10.1007/s13131-024-2336-5

1 Introduction

Submarine fans, the final site of clastic sediments, have been regarded as great potential reservoirs for oil and gas exploration (Weimer et al., 1998; Avseth et al., 2001; Fetter et al., 2009; Zhu et al., 2009; Marchand et al., 2015; He et al., 2016; Huang et al., 2017; Bello et al., 2021; Feng et al., 2021; Pandolpho et al., 2021; Zhang et al., 2021). Underground submarine fans are thus crucial to identify, classify, and analyze submarine fans' distribution and development scale according to seismic data and logging data. Source-to-sink system analysis promoted people's understanding of the formation, transportation, and deposition of submarine fan sediments and provided a better understanding of the erosion and transportation processes of clastic sediments and the associated feedback mechanisms (Tan et al., 2020; Shanmugam, 2022). The influence factors of submarine fans have been concluded, such as sea level variations, seafloor gradients, the type of continental margin, and so on(Normark et al., 1993; Reading and Richards, 1994; Bouma, 2004). According to the differences in sediment supply, submarine fans have recently been divided into two types: (1) direct-fed fans and (2) shelf- and slope-incising fans (Fisher et al., 2021). The latter commonly developed on the passive continental margin through detailed research in recent decades (Covault and Graham, 2010; Fetter et al., 2009), consistent with the northern South China Sea, so the sedimentary systems of shelf- and slope-incising fans provide an excellent example for the study herein. In other words, we draw on the experience of a depositional model of shelf- and slope-incising fans to clarify the source-to-sink system of submarine fans of the Meishan Formation in Lingshui Sag.

Submarine fans have become an essential target for oil and gas exploration in the northern South China Sea (Zhu et al., 2009; Zhang et al., 2019; Feng et al., 2021; Zhang et al., 2021), which benefits from the Pearl River deepwater fan in the Pearl (Zhujiang) River Mouth Basin and the Central Canyon in the Qiongdongnan Basin. Previous studies mainly focused on the submarine fans in Songnan-Baodao-Changchang sags in the east section of Qiongdongnan Basin and the Central Canyon in the south owing to the limit of oil and gas exploration (Zhang et al., 2016, 2017; Li et al., 2021; Sun et al., 2022), while few related studies on the submarine fans in the west of the basin. Therefore, the studied submar-

Foundation item: The National Natural Science Foundation of China under contract No. 42372154.
*Corresponding author, E-mail: fengcj@nwu.edu.cn

ine fans of the Meishan Formation in Lingshui Sag provide a reference for studying submarine fans in the western Qiongdongnan Basin and provide favourable targets and directions for oil and gas exploration in the northern South China Sea.

In this paper, 3D seismic data, logging data, and several wells were employed to: (1) identify and classify submarine fans developed in the Lingshui Sag during the Middle Miocene; (2) investigate the source-to-sink system and further clarify the sedimentary mechanism of submarine fans of the Meishan Formation in the Lingshui Sag; (3) reveal the main controlling factors that influence the morphological difference of submarine fans of the Meishan Formation in the Lingshui Sag.

2 Geological background

The Qiongdongnan Basin, geographically located in the sea area of southeast Hainan Island (16°47′–19°00′N; 108°52′–113°47′E), belongs to the Cenozoic oil- and gas-bearing basin on the northern continental margin of the South China Sea. This basin is bounded by the Yinggehai Basin with the Red River fault zone in the west and is connected with the Pearl River Mouth Basin in the east. The Qiongdongnan Basin is generally distributed in the NE–SW direction with a total area of more than 6×10^4 km^2 (Fig. 1a; Zhu et al., 2009; Qiu et al., 2013; Li et al., 2017; Zhao et al., 2018). From north to south, the basin is divided into five secondary structural units: the Northern Depression, Central Uplift, Central Depression, Southern Uplift, and Southern Depression (Fig. 1b; Huang et al., 2016; Lai et al., 2021).

The Lingshui Sag is located in the western part of the Central Depression of the Qiongdongnan Basin, with an area of about 4.6×10^3 km^2 (Fig. 1b; Zhang et al., 2016). The Lingshui Sag experienced three tectonic evolution stages, namely, the rifting stage (Tg–T60), thermal subsidence stage (T60–T40), and rapid subsidence stage (T40–T0) (Fig. 2; Lei et al., 2011; Wang et al., 2014a; Zhang et al., 2017). During the rifting stage, the Lingshui Sag extended rapidly and showed the characteristics of a half-graben with the influence of the highly active fault F2 in the Qiongdongnan Basin; at this time, the sag filled with Eocene Lingtou Formation lacustrine facies and early Oligocene Yacheng Formation lit-

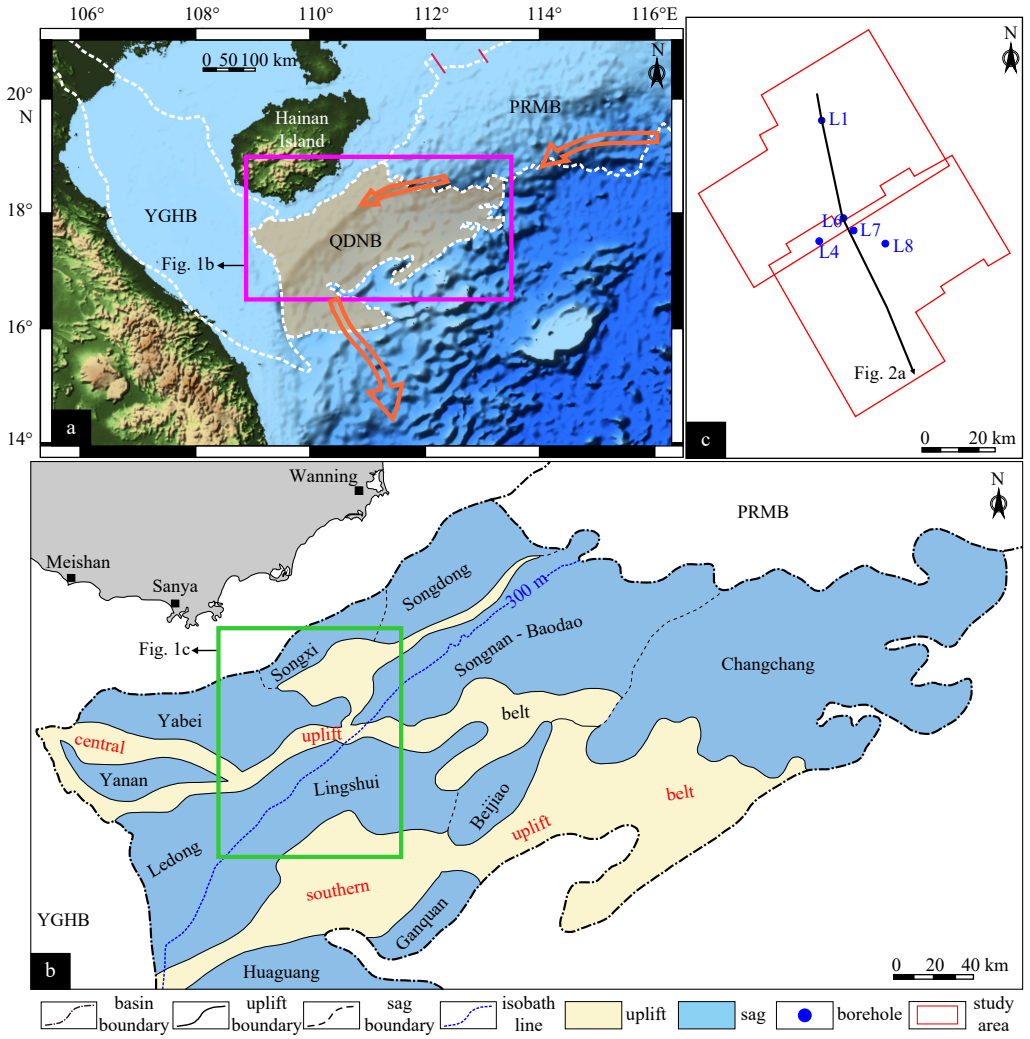

Fig. 1. The geographical location of the Qiongdongnan Basin (a); the white dashed lines represent basin boundaries; the purple rectangle represents the position of Fig. 1b; the purple arrows show the deep-water circulation in the northern South China Sea (Zheng et al., 2012; Zhao et al., 2014; Liu et al., 2016); QDNB represents the Qiongdongnan Basin; PRMB represents the Pearl River Mouth Basin; and YGHB represents the Yinggehai Basin. Figure 1b shows the plane distribution of the internal tectonic units of the Qiongdongnan Basin(Zhang et al., 2016), and the green rectangle shows the position of Fig. 1c. Figure 1c shows the coverage range of the 3D seismic data (red polygon) and the plane location of the wells used in this study.

toral-neritic facies (Northrup et al., 1995; Zhang et al., 2017). As the activity of fault F2 decreased, the subsidence center and sedimentation center of the sag migrated from fault F2 to the sag center, showing the characteristics of a fault depression and becoming filled with the neritic facies of the Lingshui Formation in the late Oligocene (Zhang et al., 2017; Liu et al., 2019). At the thermal subsidence stage, the Lingshui Sag continued to subside overall and was filled with the bathyal facies of the early Miocene Sanya Formation and Middle Miocene Meishan Formation (Zhang et al., 2016, 2017). During this period, the expansion activity of the South China Sea gradually weakened, and the reduction in sediment supply in the Qiongdongnan Basin caused sedimentation starvation, resulting in a sedimentary break in the northern Lingshui Sag (Fig. 2a; Wang et al., 2014b). At the accelerated subsidence stage, the Lingshui Sag continued to subside further and was filled with the bathyal facies of the late Miocene Huangliu Formation and Pliocene Yinggehai Formation, as well as Quaternary abyssal facies. The sedimentary strata were characterised by the seaward movement of the continental shelf, slope, and basin floor plain. The submarine fans mentioned in this paper developed in the Middle Miocene Meishan Formation with the bathyal environment (Fig. 2).

3 Data and methods

This paper uses post-stack 3D seismic reflection data and several wells (L1, L4, L6, L7, and L8) for research (Fig. 1c). The seismic data were acquired and processed by the China National Offshore Oil Corporation (CNOOC) with a standard industrial flow. Geophysical interpretation was accomplished through Geoframe software and then applied to identify the "source-to-sink" (S2S) system in the northern Lingshui Sag. The 3D seismic dataset with a high signal-to-noise ratio and resolution covers an area of nearly 4 200 km^2 total at a water depth of 556 m (Fig. 1c). The sampling interval of the seismic data is 2 ms, the bin size is 25 m × 12.5 m, and the dominant frequency is approximately 40 Hz.

The lithology and logging data (sonic, density, and gamma) were provided by CNOOC. The calibration of the top interface (T40) and bottom interface (T50) of the Meishan Formation through the synthetic seismic traces derived from the sonic and density logging curves connected the seismic reflection data with their geological significance and further indicated that seismic facies and sedimentary facies can be effectively linked.

The classical seismic stratigraphy interpretation technique proposed by Vail et al. (1977) is an efficient method used to obtain sedimentary information from seismic facies, especially in contact relationship of strata (onlap, downlap, toplap, and truncation). Identifying the contact relationship of strata herein supports the construction of the Middle Miocene strata framework at the continental shelf edge of the northern Lingshui Sag. The shelf-margin delta and submarine fan are well identified according to the use of seismic facies analysis and drilling lithology, and the application of seismic attributes is beneficial for improving the identification of seismic interpretation data, identifying seismic data anomalies (bright spot, frequency anomalies, faults, channels, etc.), and revealing potential geological information in seismic data. Among them, the amplitude attribute can effectively reveal the lithological difference, and the coherent attribute can better indicate the continuity of seismic data (Torrado et al.,

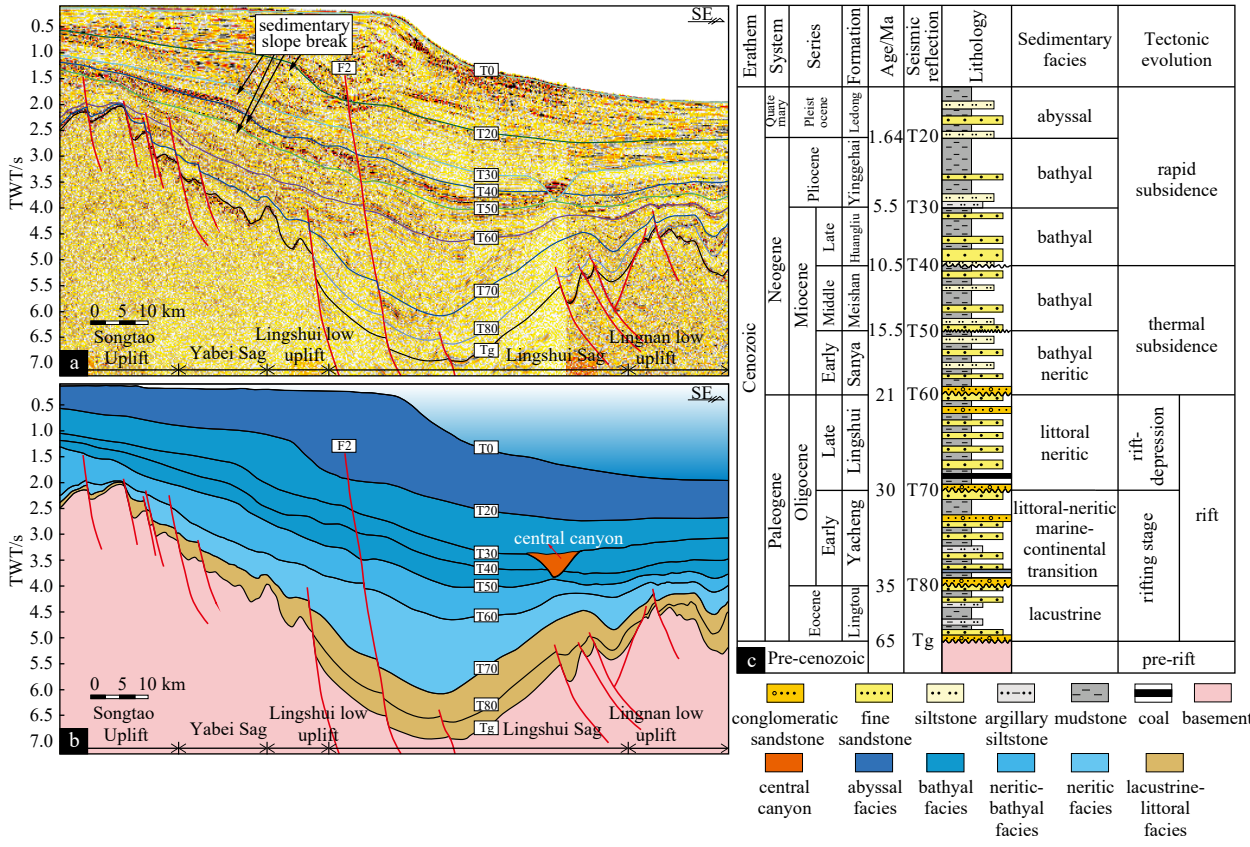

Fig. 2. The NW-SE seismic profile of the Lingshui Sag (see Fig. 1c for plane location) (a). The corresponding interpreted geological profile (b), and (c) the comprehensive histogram of the Qiongdongnan Basin (modified from Zhang et al., 2017; Sun et al., 2022).

2014; Wang et al., 2016; La Marca and Bedle, 2022). Therefore, in addition to extracting the amplitude attribute to help identify the different submarine fan plane shapes, we also extracted the coherent attribute to depict the submarine canyons in this study and achieved good results.

4 Results

4.1 *Seismic stratigraphy analysis*

4.1.1 *Seismic-well tie analysis*

Based on the borehole sonic and density logging curves, the drilling layers were calibrated on the seismic profile to obtain the corresponding relationship between the seismic data and the drilling information. Taking the calibration results of Well L1 as an example, the top interface (T40) and bottom interface (T50) of the Meishan Formation are found to be sandstone and mudstone interfaces (the mudstone is above the two interfaces, and fine sandstone is below the two interfaces). The synthetic seismic traces with zero-phased wavelets show that two interfaces (T40 and T50) are characterized by positive seismic events (shown in red on the seismic profiles), and the calibration results further reveal that a strong amplitude reflection in the Meishan Formation indicates sandy deposits, while a weak amplitude reflection indicates argillaceous deposits (Fig. 3a).

4.1.2 *Middle Miocene stratigraphy architecture in the Lingshui Sag*

The identification of the contact relationship of seismic strata is helpful for understanding the geological meaning of the stratigraphic interfaces. A downlap contact relationship indicates that the overlying strata extend toward the center of the basin, showing the progradational sequence characteristics of regression and revealing that the underlying interface is a sign of the beginning of forced regression, that is, the conformity surface CC* (Porębski and Steel, 2003; Gong et al., 2016). An onlap contact relationship indicates that the overlying strata are overlaid toward the land, showing the retrogradation sequence characteristics of transgression. At the same time, such a contact indicates that the interface where the onlap points are located is the maximum regressive surface (MRS), and a maximum flooding surface (MFS) will be formed at the end of transgression (Catuneanu, 2002; Wang et al., 2019). The regression process is usually divided into two stages (forced regression and normal regression), and the distinguishing interface between the two stages is the conformity surface CC**, which is characterized by gradual integration with the MRS in the progradation direction (Hunt and Tucker, 1992; Catuneanu et al., 1998; Figs 3a and b).

Based on the termination relationship identification of seismic strata in the Meishan Formation and Huangliu Formation, this paper reveals that a shelf margin system tract (SMST, Fig. 3) developed in the northern shelf margin of the Lingshui Sag in the Middle Miocene. The T50 interface, the first interface where the downlap points appear, corresponds to the conformity surface CC* of the bottom interface of the SMST; that is, the T50 interface represents the beginning of forced regression. Onlap points migrate continuously to the shelf of the northern Lingshui Sag on the T40 interface, meaning that the T40 interface corresponds to the MRS, showing the end of the regression phase. The T30 interface represents the MFS, indicating the end of transgression. At the same time, the conformity surface CC** is identified accord-

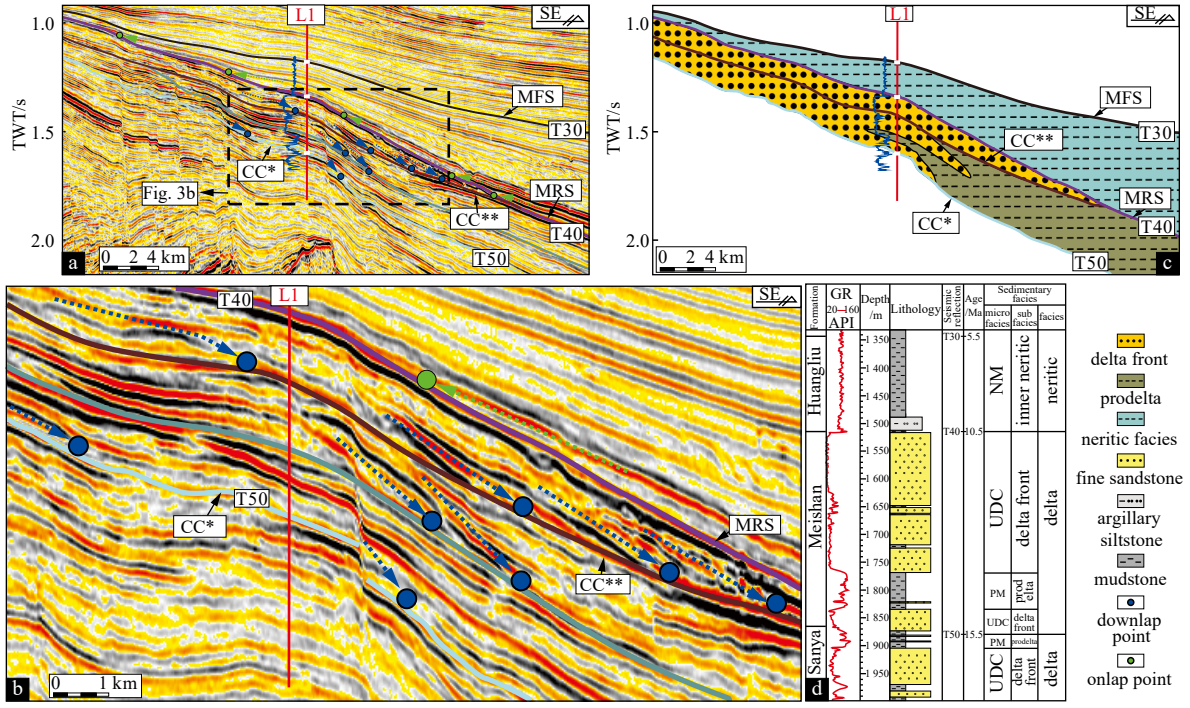

Fig. 3. Stratigraphic calibration and stratigraphy boundary identification of the Meishan Formation on the northern continental margin of Lingshui Sag. a. Shows the synthetic results of Well L1 (see Fig. 4e for the plane location); the green arrow represents the onlap, and the blue arrow represents the downlap. b. It is a locally enlarged section of Fig. 3a. c. It is the corresponding geological interpretation profile of Fig. 3a, and the blue curve is the gamma logging curve (GR). d. It is the single-well histogram of well L1. MRS represents the maximum regression surface; UDC represents the underwater distributary channel; PM represents prodelta mudstone; and NM represents neritic mudstone.

ing to the gradual integration relationship between the interface where the downlap points are located and the MRS. Identifying these characteristic interfaces clearly shows that the shelf margin system tract developed in the Middle Miocene in the northern Lingshui Sag, whereas the transgressive system tract developed in the late Miocene. The lithology of Well L1 shows that the shelf-margin delta developed in the northern Lingshui Sag during the regression period (Meishan Formation) and was dominated by thick fine sandstone deposits derived from the underwater distributary channels of the delta front, while the thick mudstone deposits composed of neritic facies developed mainly during the transgression period (Fig. 3d).

4.2 *Seismic facies and corresponding sedimentary facies*

This paper identifies five seismic facies through the comparison and analysis of the amplitude, frequency, continuity and other reflection structure parameters of seismic data from the Meishan Formation in the study area and further extracts the root mean square (RMS) amplitude attribute and coherent attribute to illustrate the plane characteristics of seismic facies in the next section (Figs 4e, 5, 6b). Moreover, the geological meaning indicated by each of the five seismic facies is defined in combination with the drilling lithology analysis. A detailed description is provided below.

4.2.1 *Seismic facies 1: Imbricated progradation seismic facies*

4.2.1.1 *Description*

The imbricated progradation seismic facies shows medium-amplitude, medium-frequency, and medium-continuity reflection. The external shape presents a wedge shape pinching out toward the center of the sag, the internal seismic events connect with the underlying interface with a low-angle downlap contact relationship, and the downlap points continuously migrate to the center of the sag, showing obvious progradation characteristics (Tables 1a and f).

4.2.1.2 *Corresponding sedimentary facies: delta*

The progradation reflection is a prominent mark of delta-front sedimentation (Pulham, 1989; Bellotti et al., 1994; Krassay and Totterdell, 2003). The imbricated progradation seismic facies develops at the shelf edge of the northern Lingshui Sag. Well L1 reveals that this facies contain the thick fine sandstones of underwater distributary channels in the delta front of the SMST developed in the Meishan Formation, with an approximate thickness of 275 m. Furthermore, during the sedimentary period of the

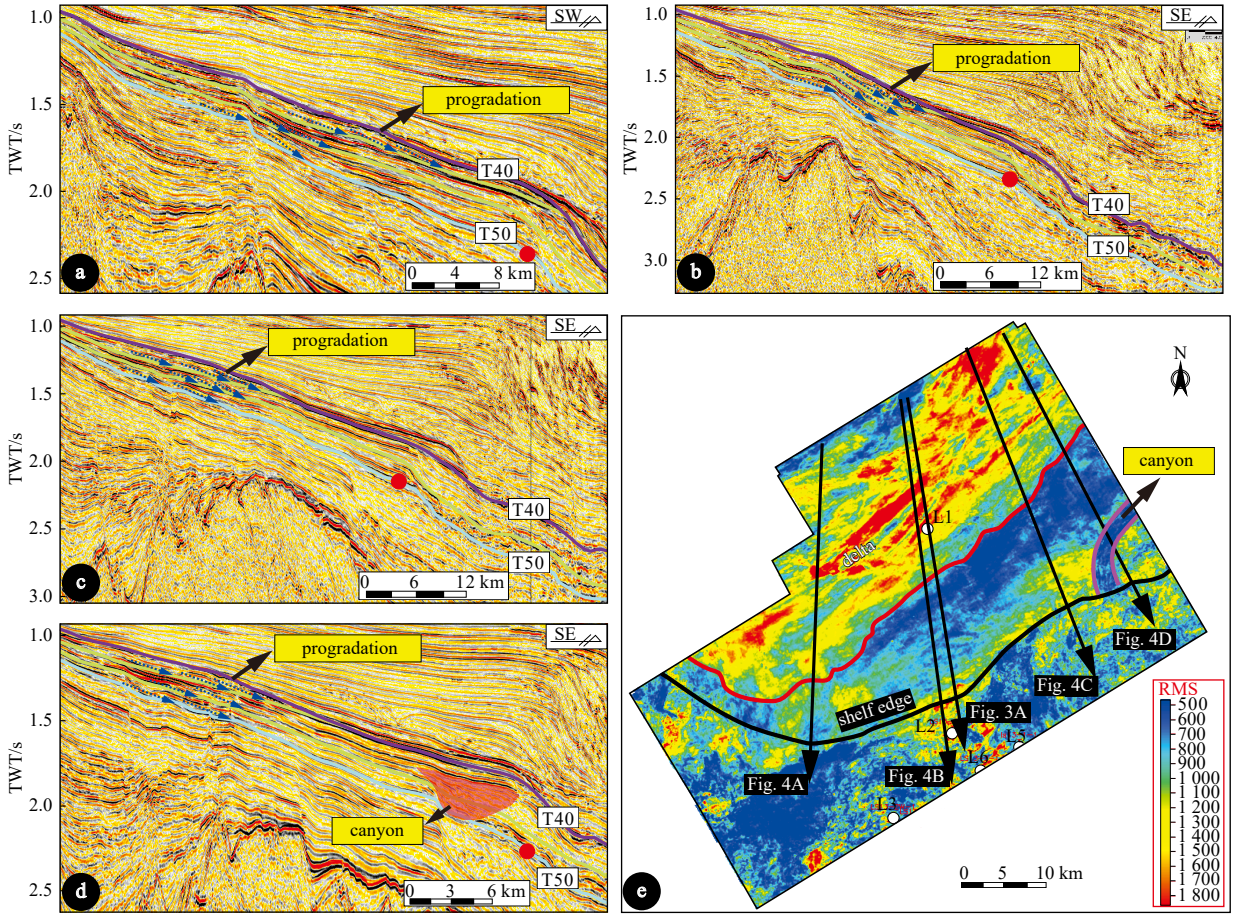

Fig. 4. Plane distribution of the continental margin delta in the northern Lingshui Sag. Panels (a), (b), (c) and (d) show seismic profiles at different locations of the continental margin delta. The blue arrow represents the downlap point position of the delta, and the red point represents the position of the shelf edge. Panel (e) is the interbedded root-mean-square amplitude attribute map of the Meishan Formation, and the red line represents the maximum extension position of the delta front, with an area of approximately 720 km^2. The purple line represents the boundary of the submarine canyon at the continental shelf; the black curve represents the position of the continental shelf edge.

Table 1. Identification results of the seismic facies of the Meishan Formation in the Lingshui Sag, Qiongdongnan Basin

Seismic facies	Seismic profile	Interpreted sketch
Imbricated progradation seismic facies	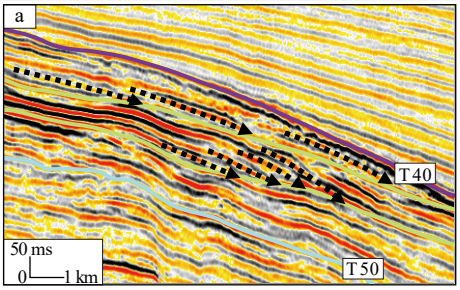	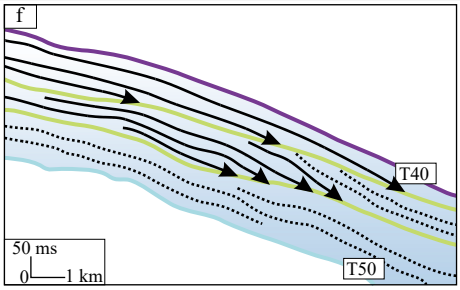
Channel-filling seismic facies	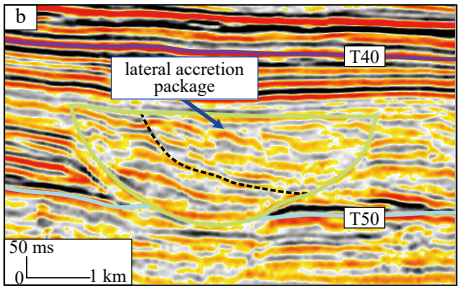	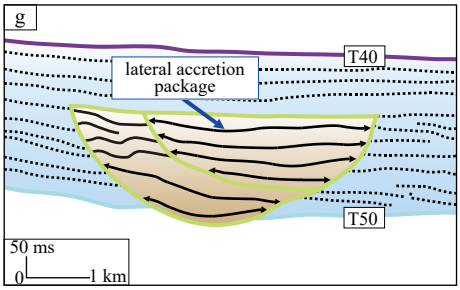
Mound-like seismic facies	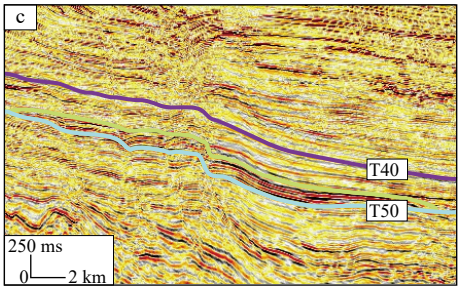	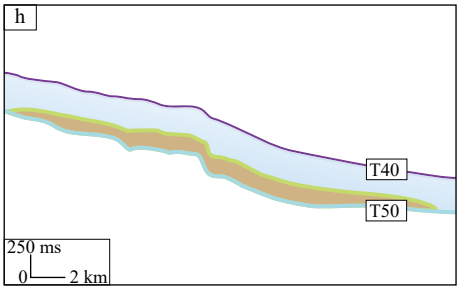
Vermicular seismic facies	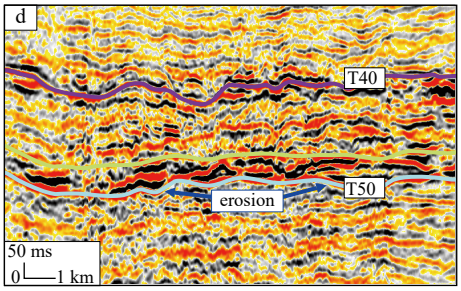	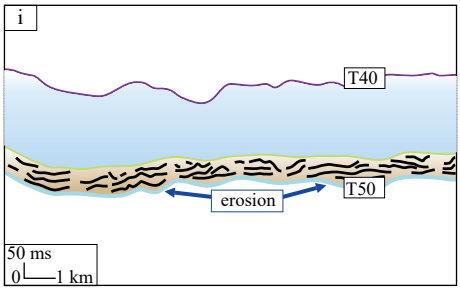
Subparallel sheet seismic facies	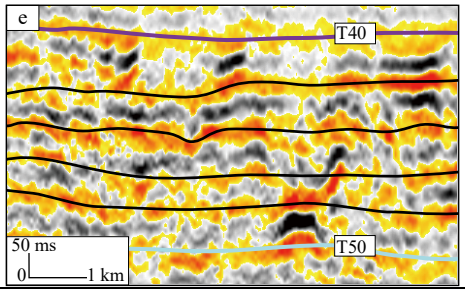	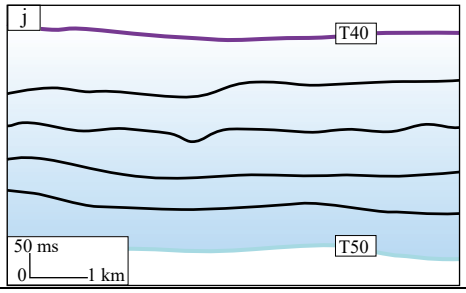

Meishan Formation, the development of a shelf-margin delta with a ratio of sandstone thickness to formation thickness greater than 0.76 indicates that the sediment source in the northern Lingshui Sag was sufficient, which was conducive to the formation of a submarine fan.

4.2.2 *Seismic facies 2: channel-filling seismic facies*

The channel-filling seismic facies presents noticeable U-shaped characteristics on the seismic profile. The top interface is flat and straight, and the bottom interface is arc-shaped and protrudes downward. Its internal reflection seismic events show weak-amplitude subparallel reflection and a two-way uplift contact with the bottom arc-shaped reflection interface (Tables 1b and g).

4.2.2.1 *Description*

The channel-filling seismic facies presents noticeable U-shaped characteristics on the seismic profile. The top interface is flat and straight, and the bottom interface is arc-shaped and protrudes downward. Its internal reflection seismic events show

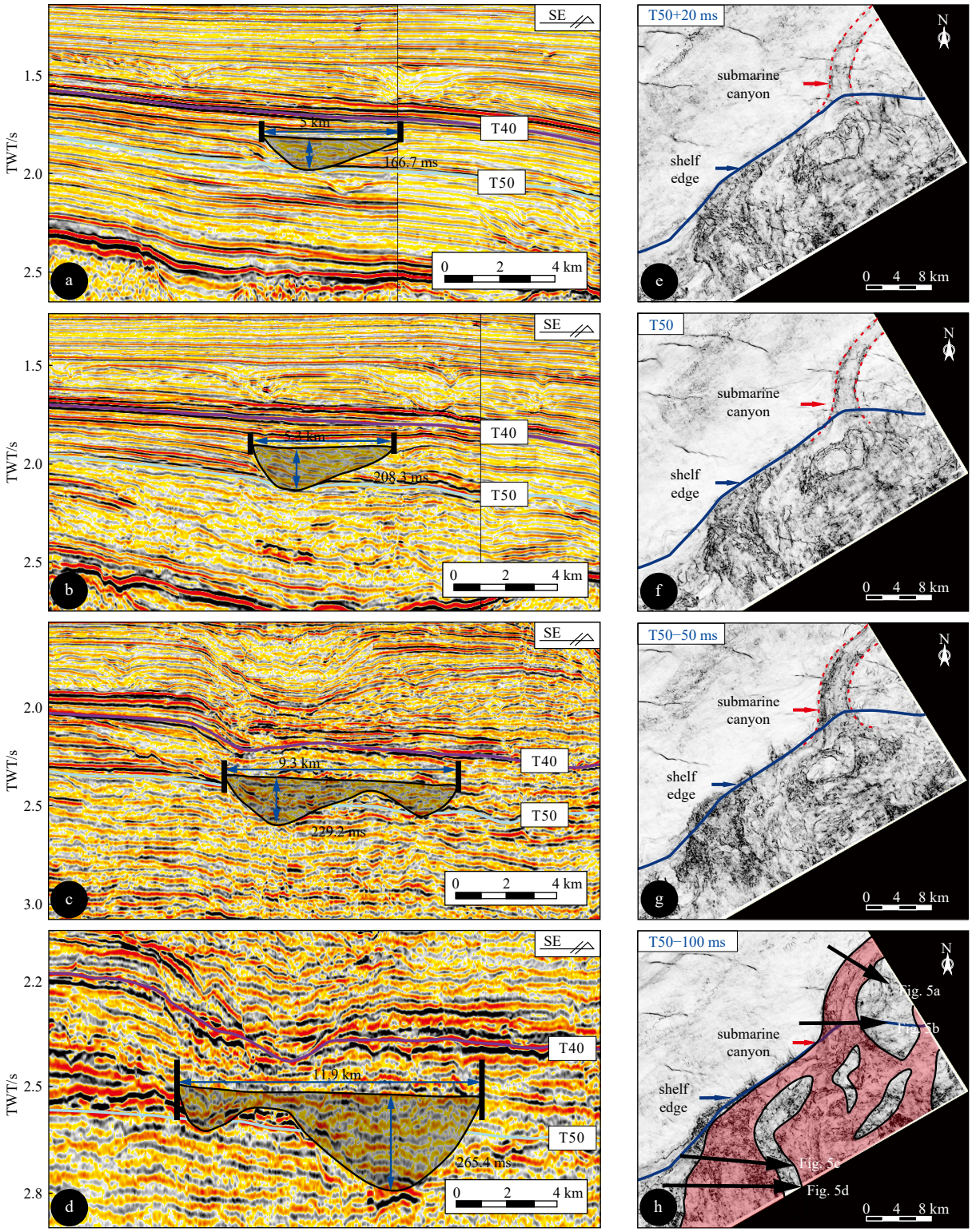

Fig. 5. Panels a, b, c and d show the seismic profiles of submarine canyon evolution in the northern Lingshui Sag (see panel (h) for the plane locations of the seismic profiles). Panels e, f, g and h show that the bottom interface T50 of the Meishan Formation shifted up and down to extract coherent slices along the layer, corresponding to +20 ms, 0 ms, –50 ms and –100 ms, respectively. The red dotted line indicates the location of the submarine canyon at the continental shelf, the blue solid line indicates the location of the continental shelf edge, and the red filled position indicates the plane distribution of submarine canyons.

weak-amplitude subparallel reflection and a two-way uplift contact with the bottom arc-shaped reflection interface (Tables 1b and g).

4.2.2.2 *Corresponding sedimentary facies: submarine conyon*

The channel-filling seismic facies found at continental shelf slope breaks usually represents typical submarine canyon identi-

fication mark (Rasmussen, 1994; Gong et al., 2011; Li et al., 2013). The channel-filling seismic facies developed at the continental shelf edge in the northern Lingshui Sag eroded the Meishan Formation and the underlying Sanya Formation strata, making the T50 interface discontinuous (Fig. 5) and showing the characteristics of lateral accretion (Table 1b); these characteristics indicate that this channel facilitated the continuous transportation of sediments. The minimum width in the transverse direction exceeds 5 km (Fig. 5), indicating the presence of a submarine canyon.

4.2.3 *Seismic facies 3: mound-like seismic facies*

4.2.3.1 *Description*

The mound-like seismic facies is characterized by strong-amplitude, medium-frequency, and medium-continuous reflection. The external shape is a mound, and four pairs of seismic events in subparallel contact are developed inside the mound and gradually thinner toward the northern continental margin and the center of the sag, exhibiting baselap characteristics. This facies spreads like a lobe from north to south on the plane (Tables 1c and h; Fig. 6).

4.2.3.2 *Corresponding sedimentary facies: lobe-shaped submarine fan*

The mound-like seismic facies is a typical seismic reflection feature of submarine fans or reefs. (Li et al., 2021; Xu and Haq, 2022). This facies has developed mainly in the center of the Lingshui Sag, corresponding to the bathyal environment during the sedimentary period of the Meishan Formation. Well L8 reveals that the lithology of this seismic facies is composed mainly of approximately 30 m thick siltstone and fine sandstone overall (Fig. 7c), indicating the presence of submarine fan deposits. Combined with the plane characteristics of the lobe, this facies is referred to as a "lobe-shaped submarine fan" hereafter.

4.2.4 *Seismic facies 4: vermicular seismic facies*

4.2.4.1 *Description*

The vermicular seismic facies is characterized by strong-amplitude, high-frequency, and poorly continuous reflection. It is mainly composed of two pairs of seismic events. The continuity of strong-amplitude seismic events is poor, showing wormlike reflection characteristics but with a robust erosive capacity. The underlying seismic events with weak amplitudes show chaotic reflections and apparent lateral thickness variations, providing direct evidence of the facies. The plane shows a northeast- to southwest-trending banded distribution (Tables 1d and i; Fig. 6).

4.2.4.2 *Corresponding sedimentary facies: band-shaped submarine fan*

The vermicular seismic facies developed closely with the continental slope of the northern Lingshui Sag, and its poor continuity corresponds to an unstable sedimentary environment (Xia et al., 2018). The drilling lithologies of wells L4, L6, and L7 show that the seismic facies are approximately 40 m to 100 m thick siltstone (Fig. 9c). The cores from Well L7 demonstrate the siltstone developed with massive bedding, which further proves this seismic facies represents a submarine fan deposit (Fig. 9f). According to the plane distribution characteristics, this facies is called a

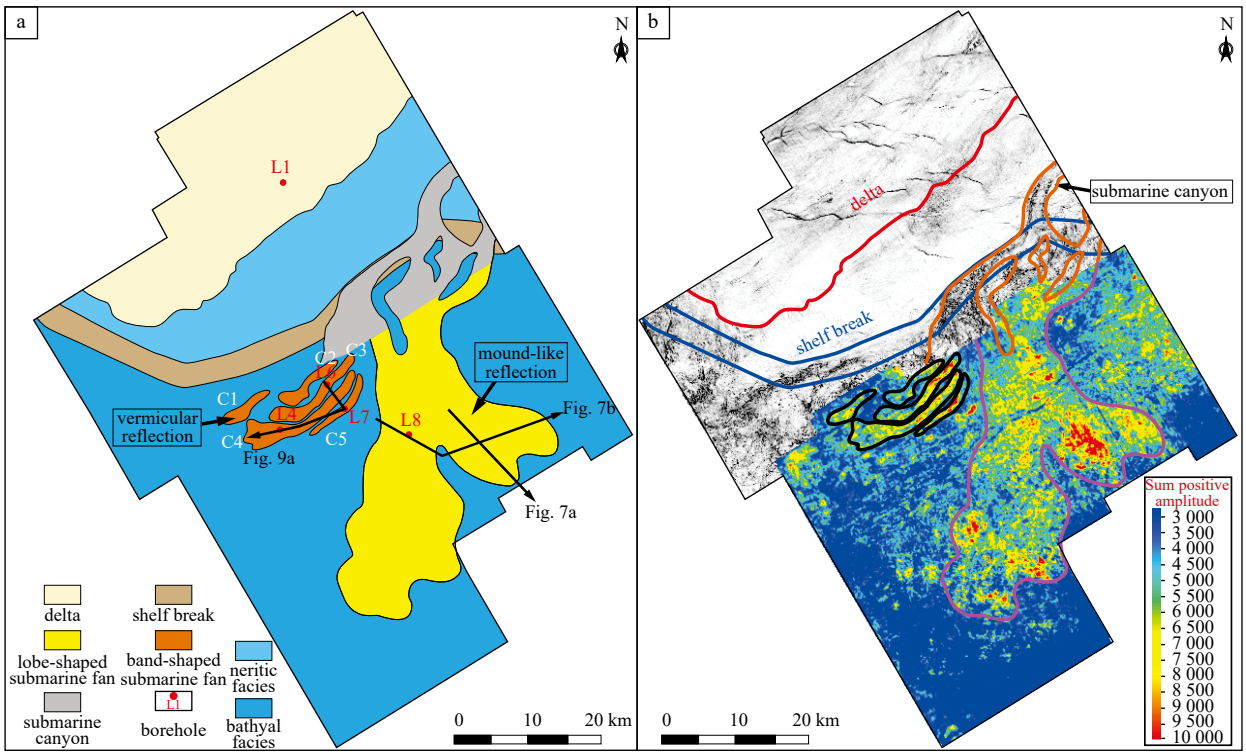

Fig. 6. Sedimentary facies of the Meishan Formation in the northern Lingshui Sag (a). The range of the submarine fan is mapped by the plane-projection transformation of the mound-like seismic facies and vermicular seismic facies; it is a superposition diagram of the maximum positive amplitude attribute map between layers (T41–T50) and coherent slices along the layers of the T50 interface (b). The red curve represents the boundary of the delta, the blue curve represents the location of the continental shelf break, the orange curve represents the boundary of the submarine canyons, the black curve represents the plane location of the vermicular seismic facies, and the purple curve represents the plane location of the mound-like seismic facies.

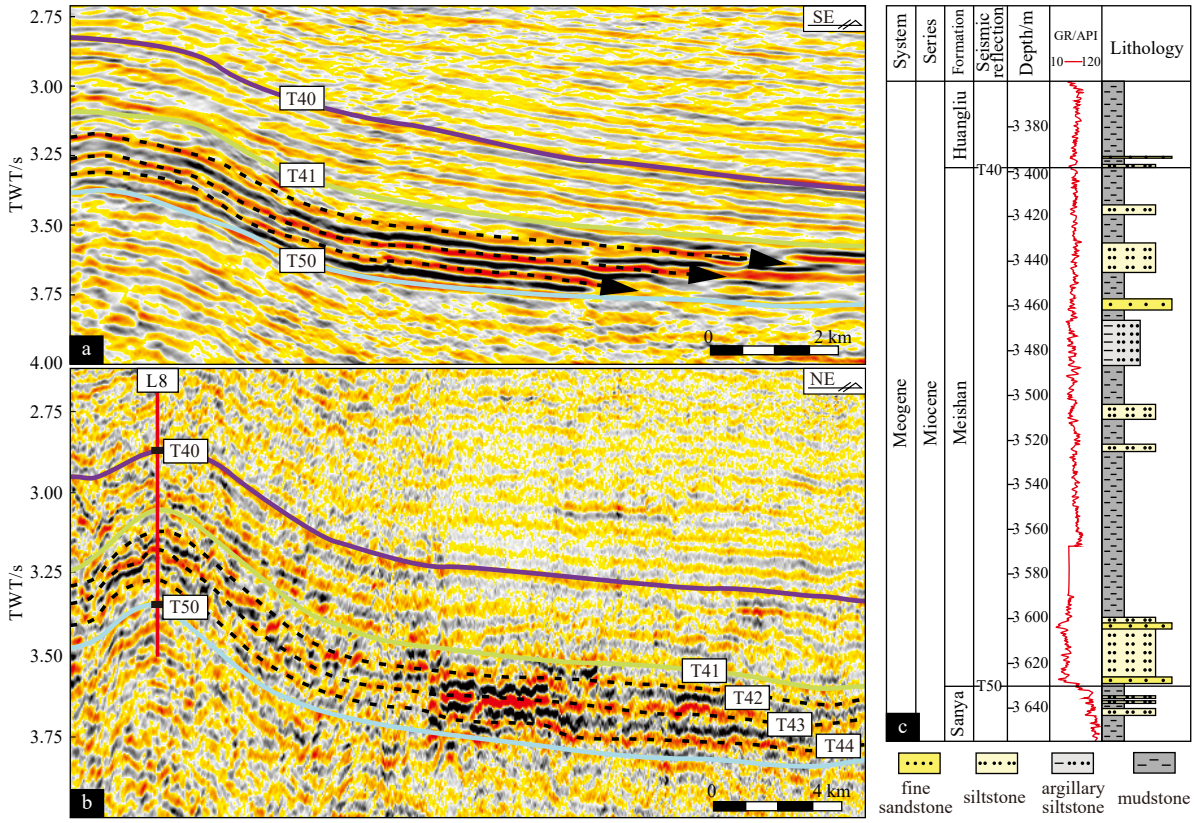

Fig. 7. Northwest-southeast-trending seismic profile of the front end of the lobe-shaped submarine fan, with the black arrow indicating the downlap position; the figure indicates that the submarine fan exhibits multiple development characteristics (see Fig. 6a for the plane location) (a). Southwest-northeast-trending lobe-shaped submarine fan seismic profile of Well L8 reveals that the lithology of the submarine fan is mainly siltstone. According to the downlap characteristics of the lobe-shaped submarine fan, four stages of submarine fan are recognized, and the interfaces are labeled T44, T43, T42, and T41 (see Fig. 6a for the plane location) (b). Lithology histogram of Well L8 (c).

"band-shaped submarine fan" hereafter (Fig. 6).

4.2.5 *Seismic facies 5: subparallel sheet seismic facies*

4.2.5.1 *Description*

The subparallel sheet seismic facies is characterized by weak-amplitude, low-frequency, and medium-continuous reflection. The seismic facies is composed of 4 pairs of seismic events in subparallel sheet contact, and the number of seismic events basically remains unchanged in the horizontal direction, indicating that the thickness changes are not obvious. This facies is widely distributed in the center of the sag (Tables 1e and j).

4.2.5.2 *Corresponding sedimentary facies: fine-grained sediments*

The weak amplitude of the subparallel sheet seismic facies reveals that the vertical difference in lithology within this facies is not obvious, and the deposits are usually deposited in a stable environment (Su et al., 2015; Li et al., 2021). A seismic facies has developed in the center of the Lingshui Sag. Well L8 is close to the development location of this seismic facies (Fig. 6), and its lithology reveals that the weak amplitude is the result of mudstone deposition (Fig. 7c). Therefore, this seismic facies mainly reflects fine-grained sediments under the stable environment of bathyal facies.

4.3 *Source-to-sink system analysis of submarine fans*

The accurate geological significance of the five typical seismic facies recognized in the Meishan Formation, northern Lingshui Sag, benefits from the comprehensive analysis of drilling lithology information and seismic data. This paper further describes the plane distribution characteristics of the Meishan Formation delta, shelf edge, submarine canyon and submarine fan in the study area by combining attribute slice analysis and seismic facies tracking interpretation methods (Figs 4, 5, 6). Based on the spatial coupling relationship of each sedimentary facies (Fig. 6), this paper considers that the deepwater source-to-sink system in the northern Lingshui Sag mainly consisted of a "delta (sediment supply) - submarine canyon (sediment transport channel) - submarine fan (sediment deepwater sink)" association during the Middle Miocene.

4.3.1 *Source: shelf-margin delta*

The shelf-margin delta is essential to the passive continental margin source-to-sink system (Gao et al., 2020; Gong et al., 2021). The imbricated progradation seismic facies (Table 1a; Fig. 4) developed at the continental shelf edge of the northern Lingshui Sag during the Middle Miocene, and the progradation seismic facies are typical identification indicators of deltas. The lithology of the Meishan Formation derived from Well L1 reveals that underwater distributary channels developed at the delta front in the northern Lingshui Sag, and the content of fine sandstone is very high in this underwater distributary channels (ratio of sandstone thickness to formation thickness exceeds 0.76, Fig. 3). The sequence stratigraphy analysis results show that during the Middle Miocene, a shelf margin system tract (SMST, regression) de-

veloped in the northern Lingshui Sag, and the trend of the downlap points extending to the center of the sag indicates that this period was conducive to the transport and deposition of sediments toward the center of the sag, while the delta progradation direction was northwest-southeast (Figs 3 and 4). The cores from Well L7 show the heavy mineral assemblages of submarine fans of Meishan Formation are mainly consist of leucoxene, tourmaline, zircon and anatase (Fig. 9e). The analysis result of heavy mineral assemblages is consistent with Hainan Uplift, which reveals the source of sediments deposited in the northern Lingshui Sag during the Middle Miocene is Hainan Uplift (Cao et al., 2013). That is, during the Middle Miocene, under the background of the development of the SMST, the sediments supplied by the Hainan Uplift continued to prograde southeastward, and a thick delta-front underwater distributary channel composed of sandstone (with a cumulative thickness of approximately 275 m) was deposited at the northern shelf edge of the Lingshui Sag. The RMS amplitude attribute shows that the delta was widely developed at the continental shelf edge with an area of 720 km^2 in the study area, and the strike was northwest-southeast (Fig. 4e). The existence of a large delta is very conducive to the development of deepwater reservoirs in the Lingshui Sag. The submarine canyons described below confirm a material supply relationship between the shelf-margin delta and the submarine fans of the Meishan Formation.

4.3.2 *Channel: submarine canyons*

Negative landforms, such as valleys and canyons, usually provide a path for sediment transportation and play a significant intermediary role between the source and sedimentation areas (Posamentier and Kolla, 2003; Ding et al., 2013). In this paper, submarine canyons with obvious channel-filling seismic facies are found to have developed on the northern continental shelf edge of the Lingshui Sag on the seismic profile; these canyons eroded the underlying stratum of the Sanya Formation, making the top interface T50 of the Sanya Formation transversely discontinuous at the submarine canyon (Figs 5a, b, c, d). Therefore, based on the T50 interface (downward drift is positive, upward drift is negative), four coherent slices along the layer were extracted, corresponding to +20 ms, 0 ms, −50 ms, and −100 ms (Figs 5e, f, g, h), and the results reveal that submarine canyons continuously developed during deposition of the Meishan Formation and that the overall trend extended from northeast to southwest. The plane position of the channel-filling seismic facies is further depicted to constrain the description of the actual development position of submarine canyons. The submarine canyon is U-shaped, with a width of approximately 5 km to 5.3 km and a time-domain thickness of approximately 166 ms to 208 ms at the shelf of northern Lingshui Sag (Figs 5a and b), which reflect that the submarine canyon experienced weak undercutting erosion. The submarine canyon at the northern continental slope of Lingshui Sag gradually diverged into a W shape and extended into Lingshui Sag, with a width of approximately 9.3 km to 11.9 km and a time-domain thickness of roughly 229 ms to 265 ms, reflecting that the gravitational potential energy was greater at the continental slope, causing the erosion of underlying strata to intensify (Figs 5c and d). The interior of the submarine canyons is characterized by weak-amplitude reflection and obvious lateral accretion (Table 1b), indicating that during the deposition of the Meishan Formation, continuous sediment transport occurred in the submarine canyon on the northern continental margin of the Lingshui Sag. The following plane coupling relationship between the submarine canyons and submarine fans confirms that the marginal submarine canyons assumed the function of transport channels of gravity flow sediments during the development of the Miocene submarine fans (Fig. 6).

4.3.3 *Sink: submarine fans*

Coarse-grained clastic sediments in deepwater environments mainly originate from submarine fans formed by gravity flow, whereas mudstone is the product of pelagic fine-grained sediments (Shanmugam et al., 1994; Hart et al., 2013; Henstra et al., 2016; Fan et al., 2021). The lithologies of wells L4, L6, L7 and L8 indicate that the sedimentary system of the Meishan Formation bathyal facies is composed mainly of mudstone and sandstone interbeds of unequal thickness (Figs 7 and 9d). At the same time, the synthetic seismic records reveal that the coarse-grained clastic sediments show strong-amplitude reflections, while the fine-grained clastic sediments show weak-amplitude reflections (Fig. 3). Therefore, the tracing interpretation of strong-amplitude reflection seismic facies and the application of amplitude attributes can reflect the sedimentary scale and morphological characteristics of the Middle Miocene submarine fans in the Lingshui Sag. The sedimentary facies plane map constructed based on the tracking and transformation of seismic facies shows that strong-amplitude vermicular seismic facies developed close to the continental slope and distributed in a northeast-southwest trend, consistent with the continental shelf and continental slope. However, mound-like seismic facies developed and extended to the center of the sag, showing a lobe-shaped distribution with a north-south trend (Fig. 6a). Taking the top interface (T41) and bottom interface (T50) of the strong-amplitude reflection of the Meishan Formation in the Lingshui Sag as the time-domain vertical window, the attribute of the maximum positive amplitude between layers was extracted, and the result is consistent with the results obtained after tracking the trend of seismic facies; that is, the strong-amplitude areas in the west are distributed in strips, and the strong-amplitude areas in the south are reflected in a lobe shape (Fig. 6b). Based on the morphological differences in submarine fans, the development types of submarine fans of the Meishan Formation in the northern Lingshui Sag are divided into lobe-shaped and band-shaped types (Fig. 6a).

4.3.3.1 *Lobe-shaped submarine fan*

The lobe-shaped submarine fan is characterized by strong-to-medium-amplitude mound-like seismic facies (Table 1c) and is distributed in a north-south trend on the plane, with two branch lobes (eastern and western) and a total area of approximately 550 km^2 (Fig. 6a). The extending ends of the seismic events show prominent downlap features (Fig. 7a). Well L8 encountered the lobe-shaped submarine fan at a well depth of 3 600 m, revealing that the lithological composition of the western branch of the submarine fan is mainly siltstone and fine sandstone deposits with a thickness of approximately 30 m (Fig. 7c). Although the eastern branch of the lobe-shaped submarine fan has not yet been drilled, the time-domain thickness of strong amplitudes and the maximum positive amplitude attribute between layers are significantly greater than those in the western branch (Figs 6b and 7b). It is thus speculated that the eastern branch of the lobe-shaped submarine fan is thicker than the western branch.

To better understand the sedimentary process of the eastern branch of the lobe-shaped submarine fan, four stages of lobe-shaped submarine fan deposition were divided based on different pinch-out locations of seismic events (Fig. 7b), and the RMS attribute was applied to reveal the distribution range of the east-

ern branch at each stage (Figs 8a, b, c, d). In the first stage (T50–T44), the eastern branch was deposited with a single lobe, covering an area of approximately 154 km^2 (Figs 8a and e). In the second stage (T44–T43), the eastern branch was deposited in two lobes at the fan margin, covering an area of approximately 192 km^2 (Figs 8b and f). In the third stage (T43–T42), the eastern branch was deposited in two lobes along the fan margin as in the second stage, covering an area of approximately 215 km^2 (Figs 8c and g). In the fourth stage (T42–T41), small lobes developed locally in the eastern branch, with a single-lobe deposit overall, covering an area of approximately 240 km^2 (Figs 8d and h). The margin of the eastern branch prograded continuously with a southeast trend during the Middle Miocene, revealing that the depositional range of the lobe-shaped submarine fan expanded toward the

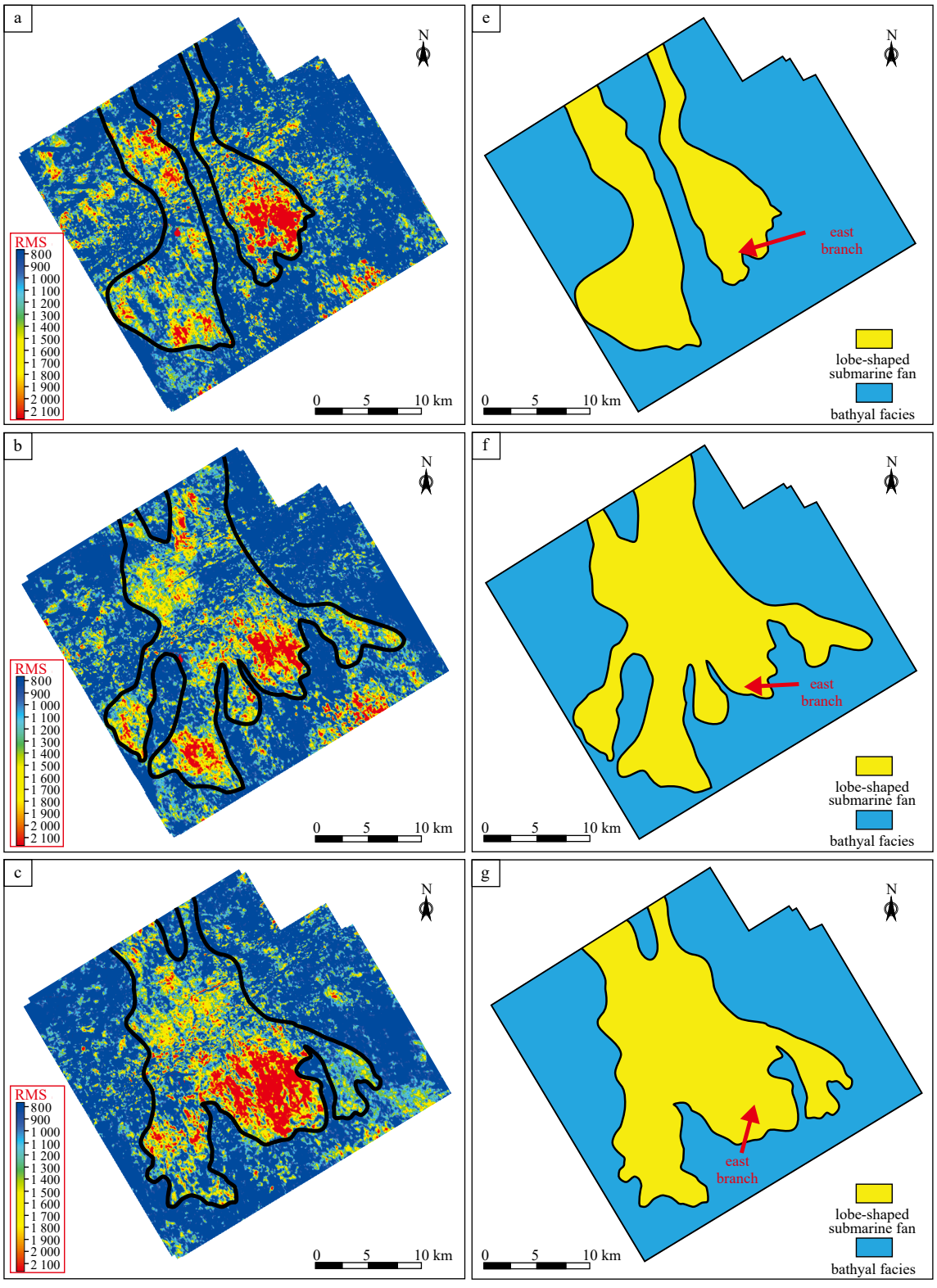

Fig. 8

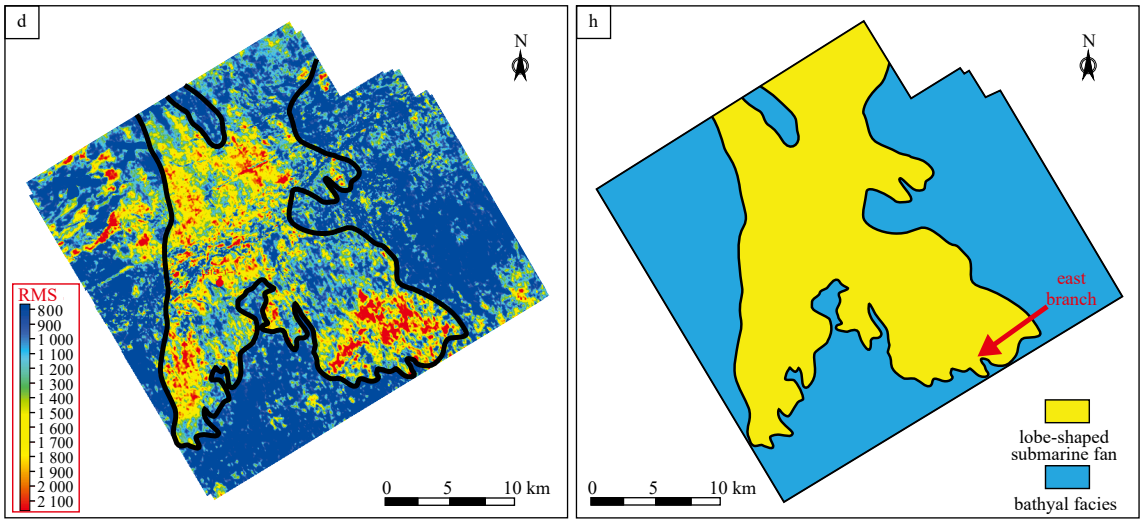

Fig. 8. Root-mean-square amplitude attributes and corresponding interpreted sedimentary facies map of each stage of the lobe-shaped submarine fan. Panels (a), (b), (c) and (d) represent the root-mean-square amplitude attribute maps of the first (T50–T44), second (T44–T43), third (T43–T42) and fourth (T42–T41) lobe-shaped submarine fans, respectively, and the purple curve represents the range of the lobe-shaped submarine fan; panels (e), (f), (g) and (h) represent the corresponding interpreted sedimentary facies maps of the first (T50–T44), second (T44–T43), third (T43–T42) and fourth (T42–T41) lobe-shaped submarine fans, respectively.

center of the sag (Fig. 8) and further reflecting that the sediment supply in the northern Lingshui Sag was sufficient during the depositional period of the Meishan Formation.

4.3.3.2 *Band-shaped submarine fan*

Five band-shaped submarine fans developed from north to south on the northern continental slope of the Lingshui Sag, and they are named C1, C2, C3, C4, and C5, with areas of approximately 18 km^2, 11 km^2, 15 km^2, 28 km^2, and 12 km^2, respectively (Fig. 6a). These fans are generally distributed in a northeast-southwest trend, consistent with the continental slope strike, with a transverse width range of 1 km to 4 km (Fig. 6a). The seismic profile shows that the band-shaped submarine fans are characterized by strong amplitude vermicular reflections and poor horizontal continuity (Figs 9a and b). C4 (depth 3 830–3 940 m), C3 (depth 3 605–3 643 m), and C5 (depth 3 775–3 814 m) were encountered in wells L4, L6, and L7, respectively, revealing that the band-shaped submarine fans are composed mainly of thick siltstone deposits (Figs 9c and d). Wells L6 and L7 are located on the northeast side of the band-shaped submarine fans, revealing that the siltstone sediment thickness of the submarine fans is approximately 40 m; Well L4 on the southwest side of the submarine fans shows that the sediment thickness of band-shaped submarine fan siltstone is about 100 m (Fig. 9d).

The development scale of band-shaped submarine fans is smaller than that of lobe-shaped submarine fans, but the siltstone thickness is larger vertically, and the thickness of a single band-shaped submarine fan gradually increases with increasing transportation distance. The following discussion will focus on the reasons for the development scales and plane distributions of these two submarine fans.

5 Discussion

5.1 *Genesis mechanism of submarine fans*

According to the analysis results of the seismic data and drilling data, this paper identified the shelf-margin delta and bathyal submarine fans developed in the northern Lingshui Sag, Qiongdongnan Basin, in the early period of the Meishan Formation. By combining the development locations of the submarine canyons and the characteristics of internal lateral accretion deposits, the deepwater source-to-sink system of a “delta (sediment supply) - submarine canyon (sediment transport channel) - submarine fan (sediment deepwater sink)” association was constructed in the Lingshui Sag, Qiongdongnan Basin in the Middle Miocene. However, the morphological description of sedimentary bodies is insufficient to explain the plane distribution and development scale differences between the band-shaped and lobe-shaped submarine fans in the northern Lingshui Sag. After analyzing the geological background of the Lingshui Sag during the Middle Miocene, it becomes clear that the relative sea level decline and seafloor gradients of the continental shelf are the main reasons for the formation of these two types of submarine fan deposits.

5.1.1 *Relative sea level decline*

The submarine fan supplied by the continental margin delta directly depends on the development scale of the delta. Essentially, it depends on the content of coarse-grained terrigenous clasts imported into the basin (Suter and Berryhill, 1985; Porębski and Steel, 2003, 2006). The theory of sequence stratigraphy shows that the clastic materials in the continental margin show progradation with the decline of relative sea level, whereas the marginal clastic materials show retrogradation characteristics when the relative sea level rises. If the relative sea level variation is not obvious, the characteristics of accretion or progradation can be observed. That is, relative sea level decline or slight variation is more conducive to transporting continental margin debris to the sedimentary center than sea level rise (Porębski and Steel, 2006; Normandeau et al., 2017; Fisher et al., 2021). Hao et al. (2000) revealed that the relative sea level of the Qiongdongnan Basin showed a downward trend in the Middle Miocene, consistent with the trend of global relative sea level variation in the Middle Miocene reported by Haq et al. (1987). Moreover, Zachos et al. 's (2008) global deep-sea foraminiferal oxygen isotope curve showed an overall increasing trend during the Middle Miocene, indicating that global sea level decline occurred during this period (Fig. 10). Most importantly, the development of the SMST in

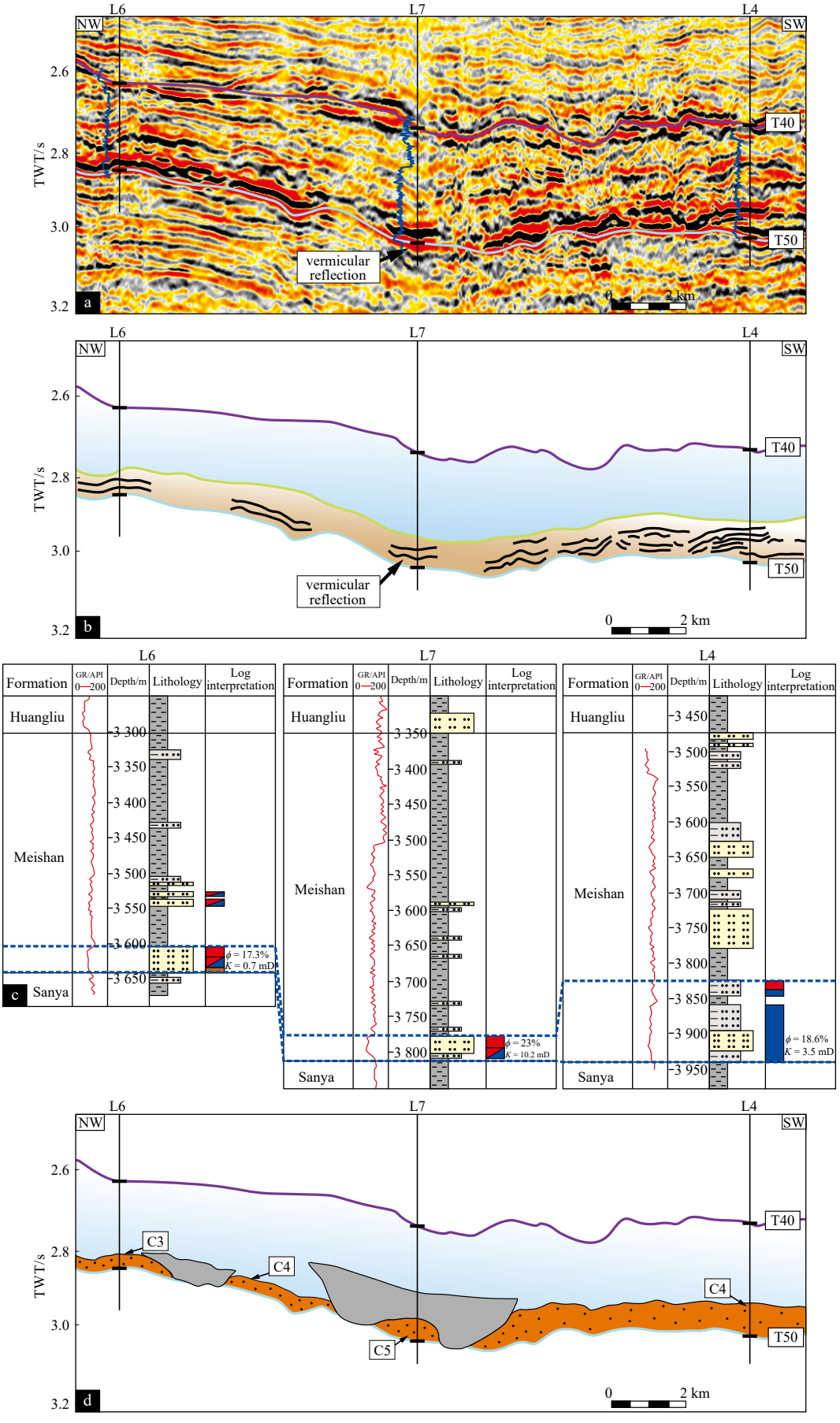
L6
L7
L4
NW
SW
TWT/s
2.6
2.8
3.0
3.2
T40
T50
vermicular reflection
0
2 km
a
b
c
d
Formation
GR/API 0—200
Depth/m
Lithology
Log interpretation
Huangliu
Meishan
Sanya
ϕ = 17.3%
K = 0.7 mD
ϕ = 23%
K = 10.2 mD
ϕ = 18.6%
K = 3.5 mD
C3
C4
C5

Fig. 9

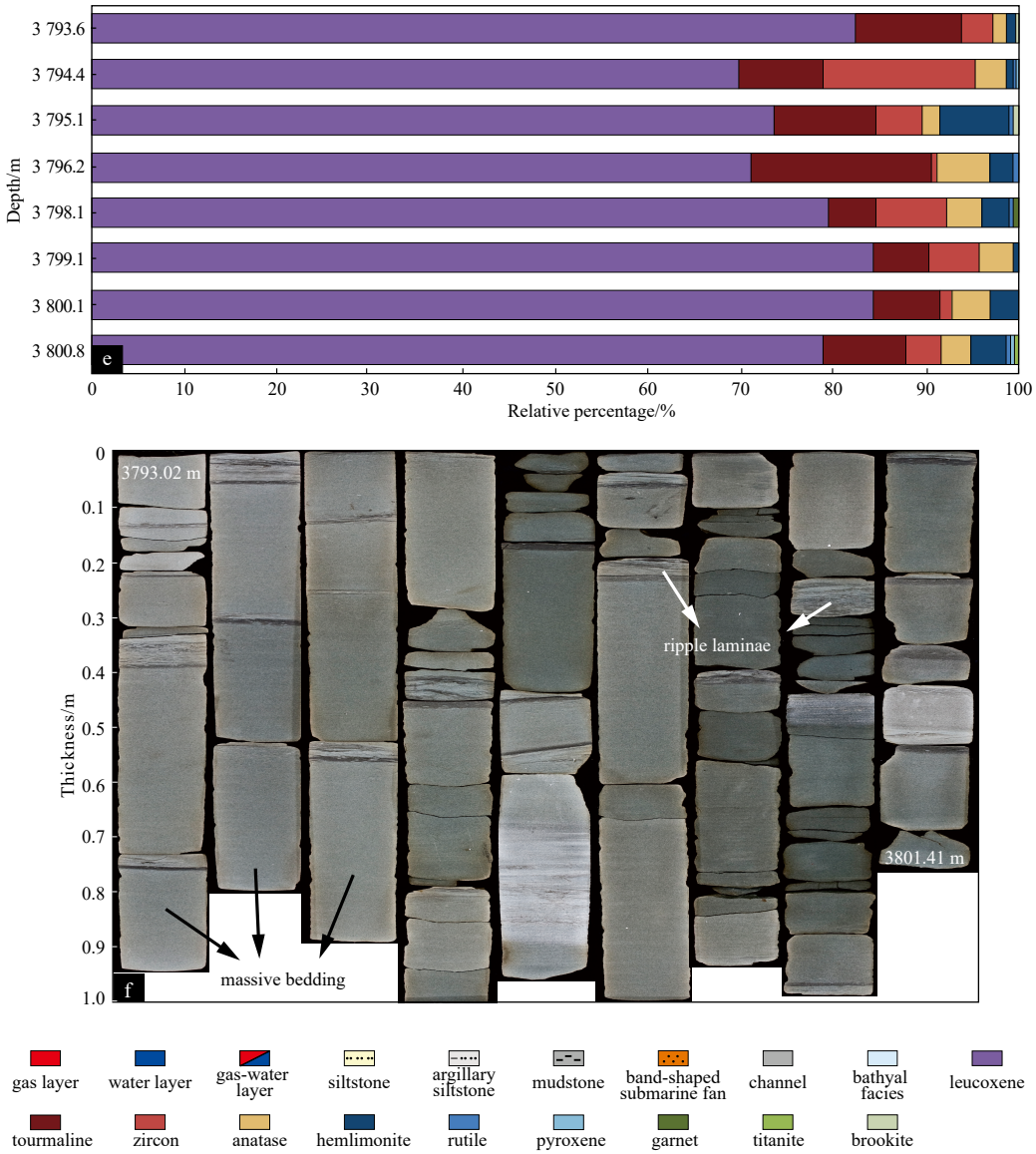

Fig. 9. Shows the seismic profile of band-shaped submarine fans through wells L6, L7 and L4. The blue curve is the gamma logging curve (GR). The submarine fan presents a strong-amplitude vermicular seismic facies. The transverse section (northwest to southeast) between wells L6 and L7 shows poor continuity of strong amplitudes, whereas the axial section (northeast to southwest) between wells L7 and L4 shows good continuity of strong amplitudes, consistent with the planar distribution characteristics of band-shaped submarine fans (see Figure 6A for the planar location) (a). It is the corresponding sketch profile of Fig.9a (b). It is a well profile of the band-shaped submarine fans of the Meishan Formation in the Lingshui Sag. The C3, C5, and C4 branches were drilled in wells L6, L7, and L4, respectively, revealing that the submarine fans consist of thick-bedded siltstone. The blue dotted line restricts the sedimentary thickness of the band-shaped submarine fans of the Meishan Formation in the Lingshui Sag. Φ represents porosity, and K represents permeability (c). It is the interpretation section of sedimentary facies corresponding to Fig.9a (d). Shows the heavy mineral assemblages in the different depth of Well L7 (e). Shows the photos of cores from Well L7 with a depth of 3 793.02–3 801.41 m, which demonstrated the band-shaped submarine fans are mainly consist of siltstone with massive bedding (f).

the northern Lingshui Sag and the continuous progradation of the marginal delta with a high sand-land ratio are direct evidence of sea level decline in the Qiongdongnan Basin in the Middle Miocene (Fig. 3), while the continuously expanding lobe-shaped submarine fan reveals the continuous transport of sediments to the Lingshui Sag during a period of relative sea level decline (Figs 7a and 8). Therefore, this paper believes that the relative sea level decline was the main factor controlling the development of the Middle Miocene submarine fan in the Lingshui Sag.

5.1.2 *Seafloor gradients*

Through comprehensive study and analysis, Zhu (2008) determined that the minimum range of the gradient that can form gravitational flow under normal geological conditions on a continental shelf is 2°–3°, but in places with gentler gradients, as long as the density of gravitationally flowing sediments is sufficiently large, the genesis mechanism can still be triggered. During the sedimentation period of the Meishan Formation, the continental shelf in the northern Lingshui Sag was less affected by tectonic activity and mainly developed sedimentary slope breaks (Figs 2a

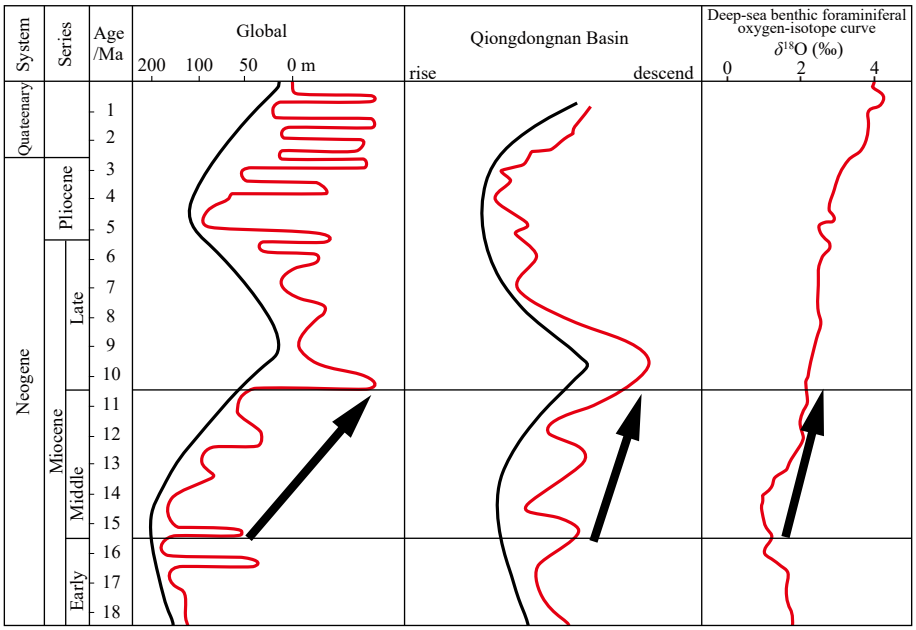

Fig. 10. Comparison of global and Qiongdongnan Basin relative sea level variations since 18.5 Ma. The black arrows indicate a continuing trend of overall sea level decline in the Middle Miocene. The global relative sea level variation is cited from Haq et al. (1987). The relative sea level variation in the Qiongdongnan Basin is cited from Hao et al. (2000). The global deep-sea foraminiferal oxygen isotope curve was modified from Zachos et al. (2008) and Zhang (2019).

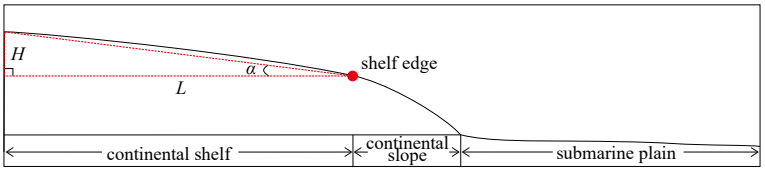

Fig. 11. Schematic diagram of the dip-angle measurement of the Middle Miocene continental shelf in the Lingshui Sag, Qiongdongnan Basin. The red dot represents the shelf-edge position, H represents the thickness, L represents the horizontal length, and α represents the dip angle of the continental shelf.

and 4). This paper established a right triangle at the shelf edge of the T50 interface to measure the horizontal length L and vertical thickness H (Fig. 11), and the angle of the shelf was calculated using the arctangent function Eq. (1). The results show that the dip angle of the continental shelf in the northern Lingshui Sag is between 2.1° and 2.9° (Table 2). Most importantly, the results reveal that the slope of the continental shelf in the northern Lingshui Sag could enable the continuous progradation of the shelf-margin delta to generate gravity flow under the background of weakening tectonic activity in the Middle Miocene, causing sediments to be transported farther from the continental slope and the center of the sag through the submarine canyons, forming the submarine fans.

$$\alpha = \arctan(H/L), \tag{1}$$

where α represents the dip angle, H represents the stratum thickness, and L represents the horizontal length of the stratum.

5.2 *Factors influencing the differences between submarine fans*

Differences were observed in the plane distribution and development scale between lobe-shaped and band-shaped submarine fans. The lobe-shaped submarine fan developed close to the center of the sag and was a lobular deposit, covering an area of approximately 550 km^2. In addition, the fan thickness was relatively thin on both sides and thick in the middle along the provenance direction, indicating the normal deposition of gravity flow in a deepwater environment (Shanmugam, 2016). The band-shaped submarine fan developed close to the continental slope and had the same trend as the continental slope, showing a northeast-southwest strip-oriented distribution and extending direction perpendicularly to the provenance direction, with a total area of approximately 80 km^2. The drilling lithology results reveal that the sedimentary thickness gradually increased with an increasing transport distance (from 40 m to 100 m; Fig. 9).

Table 2. Dip-angle statistics of the continental shelf in the northern Lingshui Sag.

Measuring position	H (vertical thickness)/m	L (horizontal length)/m	α (dip angle)/(°)
Fig. 4a	837	21 000	2.3
Fig. 4b	798	16 900	2.7
Fig. 4c	858	22 900	2.1
Fig. 4d	1 153	22 300	2.9

5.2.1 *Factor influencing the morphological difference*

This paper considers that the bottom current of the northern South China Sea reworked the sediments of the lobe-shaped submarine fan developed in the northern slope of Lingshui Sag, and then the band-shaped submarine fan formed and distributed

parallel to the continental slope. Previous studies have demonstrated that Northern Pacific Deep Water (NPDW) flows into the Luzon strait, which further evolves into the bottom current in the northern South China Sea (Wang et al., 2023). The bottom current in the northern South China Sea circled in a counterclockwise direction (Shao et al., 2007; Zheng et al., 2012; Zheng and Yan, 2012; Zhao et al., 2014; Liu et al., 2016; Fig. 1a), which is consistent with the trend of the band-shaped submarine fan. So the bottom current could transform the submarine fans. In addition, seismic profiles from wells L6 and L7 show that weak-amplitude channels existed in the same direction as the bottom current and eroded the lobe-shaped submarine fan (Figs 9a and d), which also explains the poorly continuous vermicular seismic facies of the band-shaped submarine fan. It is concluded that the bottom current in the northern South China Sea destroyed and transported the sediments of the submarine fans in the northern slope of the Lingshui Sag in the Middle Miocene, converting the lobe-shaped submarine fan into a band-shaped submarine fan. Correspondingly, the lobe-shaped submarine fan in the east has not been reconstructed because it is far from the continental slope.

5.2.2 *Factor influencing the development scale difference*

This paper considers that the angle between the direction of gravitational flow and the strike of the continental slope controlled the difference in the development scale of the submarine fans. According to Eq. (2), the component force (F) of the sediment gravity along the moving direction was influenced by the magnitude of slope (θ) (the greater the slope was, the greater the component force was). Therefore, since the dip angle of the continental slope was greater than that of the continental shelf, the moving speed of sediments under gravitational flow on the continental slope further increased. On the other hand, the greater the angle (λ) between the direction of sediment gravity flow and the strike of the continental slope was (the maximum possible value is 90°, that is, perpendicular to the strike of the continental slope), the greater the dip angle of the slope (θ) was along the direction of gravity flow movement and the more gradual the dip angle of the slope close to the maximum slope (β) was. In other words, the larger the angle between the slope and the orientation of gravitational flow (λ) was, the greater the increase of the gravity flow velocity at the continental slope was, and therefore the farther the sediments could be transported (Fig. 12). Since the included angle between the lobe-shaped submarine fan and the continental slope strike was larger than that between the band-shaped submarine fan and the continental slope strike (Fig. 6), the gravity flow sediments forming the lobe-shaped submarine fan moved faster and could be transported farther. This paper proposes that this is why the depositional range of the lobe-shaped submarine fan was larger than that of the band-shaped submarine fan.

$$F = G \cdot \sin\theta, \tag{2}$$

where F represents the force component of gravity along the direction of movement, G represents gravity, θ represents the slope of the dip angle.

5.3 *Depositional model*

Based on the analysis of the source-to-sink system of the Middle Miocene submarine fans in the Lingshui Sag and the discussion of their genesis mechanisms, this paper proposes the following sedimentary model of the Middle Miocene submarine fans in the Lingshui Sag: the relative sea level decline in the northern South China Sea resulted in the continuous progradation of the shelf-margin delta, and the sediments of the delta front produced a gravity flow of specific scale under the influence of their mass and the seafloor gradients. The gravity flow sediments were transported through submarine canyons and deposited near the continental slope and the center of the sag, developing lobe-shaped submarine fans. The later activity of bottom currents in the northern South China Sea transformed the lobe-shaped submarine fan near the continental slope, thus forming a northeast-southwest-trending band-shaped submarine fan (Fig. 13).

5.4 *Oil and gas exploration value*

The logging interpretation results show that the band-shaped submarine fan sandstone of the Meishan Formation displays natural gas, medium porosity (17.3%–23%), and low-to-medium permeability (0.7 mD–10.2 mD), confirming that the band-shaped submarine fans of the Lingshui Sag have an excellent reservoir and reservoir-forming capacities (Fig. 9c). The lithology of the lobe-shaped submarine fan is consistent with that of the band-shaped submarine fan, and the lobe-shaped fan is located

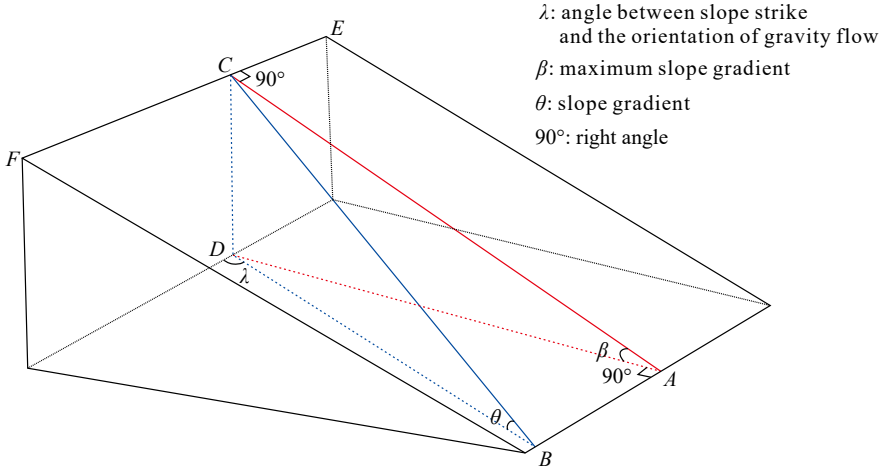

Fig. 12. Schematic diagram of gravity flow velocity differences. *AC* represents the direction of gravity flow perpendicular to the strike of the continental slope, *BC* represents the direction of gravity flow with an acute angle between the direction and the strike of the continental slope, and *EF* represents the strike of the continental slope.

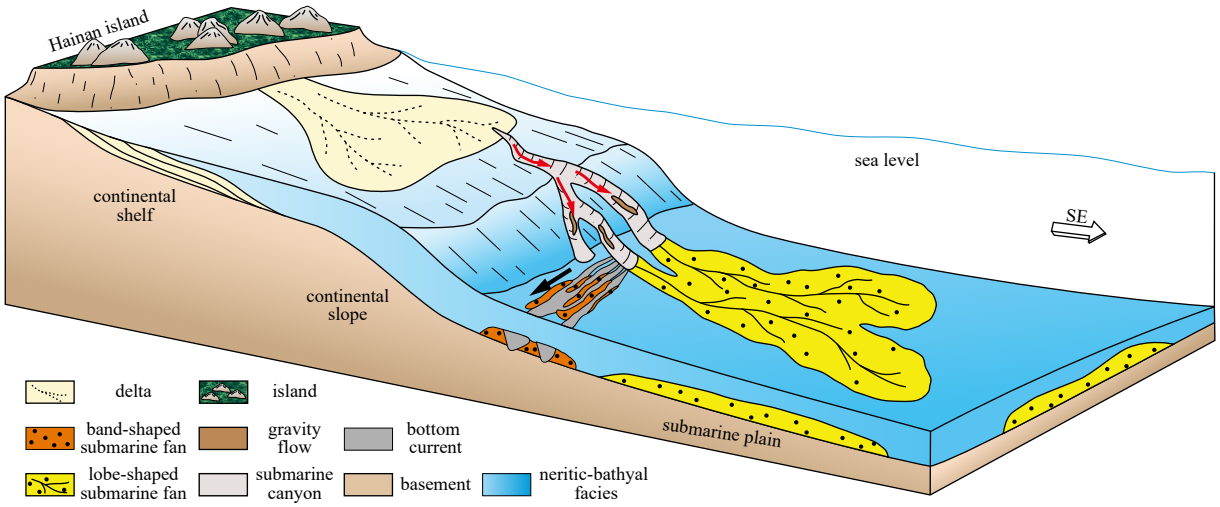

Fig. 13. Sedimentary model of Middle Miocene submarine fans in the Lingshui Sag. The red arrows represent the direction of gravity flow sediments; the black arrow represents the moving direction of the bottom current.

closer to the center of the sag (Fig. 6), compatible with the geological conditions necessary for the formation of natural gas; thus, this submarine fan should be considered for further oil and gas exploration.

6 Conclusions

Based on the analysis results of the source-to-sink system and genesis mechanisms of Middle Miocene submarine fans in the northern Lingshui Sag, the following conclusions were obtained:

(1) Two types of submarine fans with distinct morphological differences in the Meishan Formation in the northern Lingshui Sag were identified, namely, lobe-shaped and band-shaped submarine fans. The lithology of the submarine fans is dominated by siltstone with massive bedding and ripple laminae.

(2) The deepwater source-to-sink system of the Meishan Formation in the northern Lingshui Sag consists of a "delta (sediment supply) - submarine canyon (sediment transport channel) - submarine fan (sediment deepwater sink)" association. The relative sea level decline was the main factor controlling the development of the submarine fans, ensuring adequate sediments were supplied to the Lingshui Sag in the Middle Miocene.

(3) The bottom current in the northern South China Sea was the main factor that resulted in the morphological difference of submarine fans of the Meishan Formation in the Lingshui Sag. The bottom current reworked the lobe-shaped submarine fan deposited on the continental slope, forming the band-shaped submarine fan with the northeast-southwest trend.

Acknowledgements

We thank China National Offshore Oil Corporation(CNOOC) for providing seismic data and other necessary data. We are grateful to two anonymous reviewers for their insightful and constructive comments, all of which significantly improved the overall quantity of this research.

References

Avseth P, Mukerji T, Jørstad A, et al. 2001. Seismic reservoir mapping from 3-D AVO in a North Sea turbidite system. Geophysics, 66(4): 1157–1176, doi: 10.1190/1.1487063

Bello A M, Jones S, Gluyas J, et al. 2021. Role played by clay content in controlling reservoir quality of submarine fan system, Forties Sandstone Member, Central Graben, North Sea. Marine and Petroleum Geology, 128: 105058, doi: 10.1016/j.marpetgeo.2021.105058

Bellotti P, Chiocci F L, Milli S, et al. 1994. Sequence stratigraphy and depositional setting of the Tiber Delta: integration of high-resolution seismics, well logs, and archeological data. Journal of Sedimentary Research, 64(3b): 416–432

Bouma A H. 2004. Key controls on the characteristics of turbidite systems. In: Lomas S A, Joseph P, eds. Confined Turbidite Systems. London: Geological Society of London, 9–22

Cao Licheng, Jiang Tao, Wang Zhenfeng, et al. 2013. Characteristics of heavy minerals and their implications for Neogene provenances evolution in Qiongdongnan Basin. Journal of Central South University (Science and Technology) (in Chinese), 44(5): 1971–1981

Catuneanu O. 2002. Sequence stratigraphy of clastic systems: concepts, merits, and pitfalls. Journal of African Earth Sciences, 35(1): 1–43, doi: 10.1016/S0899-5362(02)00004-0

Catuneanu O, Willis A J, Miall A D. 1998. Temporal significance of sequence boundaries. Sedimentary Geology, 121(3–4): 157–178, doi: 10.1016/S0037-0738(98)00084-0

Covault J A, Graham S A. 2010. Submarine fans at all sea-level stands: tectono-morphologic and climatic controls on terrigenous sediment delivery to the deep sea. Geology, 38(10): 939–942, doi: 10.1130/G31081.1

Ding Weiwei, Li Jiabiao, Li Jun, et al. 2013. Morphotectonics and evolutionary controls on the Pearl River canyon system, South China Sea. Marine Geophysical Research, 34(3–4): 221–238, doi: 10.1007/s11001-013-9173-9

Fan Caiwei, Xu Changgui, XU Jie. 2021. Genesis and characteristics of Miocene deep-water clastic rocks in Yinggehai and Qiongdongnan Basins, Northern South China Sea. Acta Geologica Sinica (English Edition), 95(1): 153–166, doi: 10.1111/1755-6724.14637

Feng Congjun, Yao Xingzong, Yang Haizhang, et al. 2021. Source-sink system and sedimentary model of progradational fan delta controlled by restricted ancient gully: an example in the Enping Formation in the Southern Baiyun Sag, Pearl River Mouth Basin, Northern South China Sea. Acta Geologica Sinica (English Edition), 95(1): 232–247, doi: 10.1111/1755-6724.14627

Fetter M, De Ros L F, Bruhn C H L. 2009. Petrographic and seismic evidence for the depositional setting of giant turbidite reservoirs and the paleogeographic evolution of Campos Basin, offshore Brazil. Marine and Petroleum Geology, 26(6): 824–853, doi: 10.1016/j.marpetgeo.2008.07.008

Fisher W L, Galloway W E, Steel R J, et al. 2021. Deep-water depositional systems supplied by shelf-incising submarine canyons: recognition and significance in the geologic record. Earth-Science Reviews, 214: 103531, doi: 10.1016/j.earscirev.2021.103531

Gao Mengtian, Xu Shang, Zhuo Haiteng, et al. 2020. Coupling rela-

tionship between shelf-edge trajectories and slope morphology and its implications for deep-water oil and gas exploration: a case study from the passive continental margin, East Africa. Journal of Earth Science, 31(4): 820–833, doi: 10.1007/s12583-020-1288-8

Gong Chenglin, Li Dongwei, Steel R J, et al. 2021. Delta-to-fan source-to-sink coupling as a fundamental control on the delivery of coarse clastics to deepwater: insights from stratigraphic forward modelling. Basin Research, 33(6): 2960–2983, doi: 10.1111/bre.12591

Gong Chenglin, Steel R J, Wang Yingmin, et al. 2016. Shelf-margin architecture variability and its role in sediment-budget partitioning into deep-water areas. Earth-Science Reviews, 154: 72–101, doi: 10.1016/j.earscirev.2015.12.003

Gong Chenglin, Wang Yingmin, Zhu Weilin, et al. 2011. The Central Submarine Canyon in the Qiongdongnan Basin, northwestern South China Sea: architecture, sequence stratigraphy, and depositional processes. Marine and Petroleum Geology, 28(9): 1690–1702, doi: 10.1016/j.marpetgeo.2011.06.005

Hao Yichun, Chen Pingfu, Wan Xiaoqiao, et al. 2000. Late Tertiary sequence stratigraphy and sea level changes in Yinggehai-Qiongdongnan Basin. Geoscience (in Chinese), 14(3): 237–245

Haq B U, Hardenbol J, Vail P R. 1987. Chronology of fluctuating sea levels since the Triassic. Science, 235(4793): 1156–1167, doi: 10.1126/science.235.4793.1156

Hart B S, Macquaker J H S, Taylor K G. 2013. Mudstone ("shale") depositional and diagenetic processes: Implications for seismic analyses of source-rock reservoirs. Interpretation, 1(1): B7–B26, doi: 10.1190/INT-2013-0003.1

He Dashuang, Hou Dujie, Zhang Penghui, et al. 2016. Reservoir characteristics in the LW3–1 structure in the deepwater area of the Baiyun sag, South China Sea. Arabian Journal of Geosciences, 9(4): 251, doi: 10.1007/s12517-015-2279-4

Henstra G A, Grundvåg S A, Johannessen E P, et al. 2016. Depositional processes and stratigraphic architecture within a coarse-grained rift-margin turbidite system: the Wollaston Forland Group, east Greenland. Marine and Petroleum Geology, 76: 187–209, doi: 10.1016/j.marpetgeo.2016.05.018

Huang Heting, Huang Baojia, Huang Yiwen, et al. 2017. Condensate origin and hydrocarbon accumulation mechanism of the deepwater giant gas field in western South China Sea: a case study of Lingshui 17–2 gas field in Qiongdongnan Basin. Petroleum Exploration and Development, 44(3): 409–417, doi: 10.1016/S1876-3804(17)30047-2

Huang Baojia, Tian Hui, Li Xushen, et al. 2016. Geochemistry, origin and accumulation of natural gases in the deepwater area of the Qiongdongnan Basin, South China Sea. Marine and Petroleum Geology, 72: 254–267, doi: 10.1016/j.marpetgeo.2016.02.007

Hunt D, Tucker M E. 1992. Stranded parasequences and the forced regressive wedge systems tract: deposition during base-level' fall. Sedimentary Geology, 81(1-2): 1–9, doi: 10.1016/0037-0738(92)90052-S

Krassay A A, Totterdell J M. 2003. Seismic stratigraphy of a large, Cretaceous shelf-margin delta complex, offshore southern Australia. AAPG Bulletin, 87(6): 935–963, doi: 10.1306/01240300015

La Marca K, Bedle H. 2022. Deepwater seismic facies and architectural element interpretation aided with unsupervised machine learning techniques: Taranaki basin, New Zealand. Marine and Petroleum Geology, 136: 105427, doi: 10.1016/j.marpetgeo.2021.105427

Lai Hongfei, Fang Yunxin, Kuang Zenggui, et al. 2021. Geochemistry, origin and accumulation of natural gas hydrates in the Qiongdongnan Basin, South China Sea: implications from site GMGS5-W08. Marine and Petroleum Geology, 123: 104774, doi: 10.1016/j.marpetgeo.2020.104774

Lei Chao, Ren Jianye, Li Xushen, et al. 2011. Structural characteristics and petroleum exploration potential in the deep-water area of the Qiongdongnan Basin, South China Sea. Petroleum Exploration and Development (in Chinese), 38(5): 560–569

Li Chao, Chen Guojun, Zhou Qianshan, et al. 2021. Seismic geomorphology of three types of deepwater fans and their relationship with slope morphology: Qiongdongnan Basin, northern South China Sea. Marine and Petroleum Geology, 124: 104814, doi: 10.1016/j.marpetgeo.2020.104814

Li Xiangquan, Fairweather L, Wu Shiguo, et al. 2013. Morphology, sedimentary features and evolution of a large palaeo submarine canyon in Qiongdongnan basin, Northern South China Sea. Journal of Asian Earth Sciences, 62: 685–696, doi: 10.1016/j.jseaes.2012.11.019

Li Chao, Lv Chengfu, Chen Guojun, et al. 2017. Source and sink characteristics of the continental slope-parallel Central Canyon in the Qiongdongnan Basin on the northern margin of the South China Sea. Journal of Asian Earth Sciences, 134: 1–12, doi: 10.1016/j.jseaes.2016.10.014

Liu Shiyou, Chen Hongyan, Li Deyong, et al. 2019. Sedimentary characteristics and source rock development model of the Oligocene Lingshui Formation in Lingshui Sag, Qiongdongnan Basin. Marine Origin Petroleum Geology (in Chinese), 24(1): 63–70

Liu Zhifei, Zhao Yulong, Colin C, et al. 2016. Source-to-sink transport processes of fluvial sediments in the South China Sea. Earth-Science Reviews, 153: 238–273, doi: 10.1016/j.earscirev.2015.08.005

Marchand A M E, Apps G, Li Weiguo, et al. 2015. Depositional processes and impact on reservoir quality in deepwater Paleogene reservoirs, US Gulf of Mexico. AAPG Bulletin, 99(9): 1635–1648, doi: 10.1306/04091514189

Normandeau A, Dietrich P, Lajeunesse P, et al. 2017. Timing and controls on the delivery of coarse sediment to deltas and submarine fans on a formerly glaciated coast and shelf. GSA Bulletin, 129(11–12): 1424–1441

Normark W R, Posamentier H, Mutti E. 1993. Turbidite systems: state of the art and future directions. Reviews of Geophysics, 31(2): 91–116, doi: 10.1029/93RG02832

Northrup C J, Royden L H, Burchfiel B C. 1995. Motion of the Pacific plate relative to Eurasia and its potential relation to Cenozoic extension along the eastern margin of Eurasia. Geology, 23(8): 719–722, doi: 10.1130/0091-7613(1995)023<0719:MOTPPR>2.3.CO;2

Pandolpho B T, da Fontoura Klein A H, Dutra I, et al. 2021. Seismic record of a cyclic turbidite-contourite system in the Northern Campos Basin, SE Brazil. Marine Geology, 434: 106422, doi: 10.1016/j.margeo.2021.106422

Porębski S J, Steel R J. 2003. Shelf-margin deltas: their stratigraphic significance and relation to deepwater sands. Earth-Science Reviews, 62(3–4): 283–326, doi: 10.1016/S0012-8252(02)00161-7

Porębski S J, Steel R J. 2006. Deltas and sea-level change. Journal of Sedimentary Research, 76(3): 390–403, doi: 10.2110/jsr.2006.034

Posamentier H W, Kolla V. 2003. Seismic geomorphology and stratigraphy of depositional elements in deep-water settings. Journal of Sedimentary Research, 73(3): 367–388, doi: 10.1306/111302730367

Pulham A J. 1989. Controls on internal structure and architecture of sandstone bodies within Upper Carboniferous fluvial-dominated deltas, County Clare, western Ireland. Geological Society, London, Special Publications, 41(1): 179–203

Qiu Ning, Wang Zhenfeng, Xie Hui, et al. 2013. Geophysical investigations of crust-scale structural model of the Qiongdongnan Basin, Northern South China Sea. Marine Geophysical Research, 34(3): 259–279

Rasmussen E S. 1994. The relationship between submarine canyon fill and sea-level change: an example from Middle Miocene offshore Gabon, West Africa. Sedimentary Geology, 90(1–2): 61–75, doi: 10.1016/0037-0738(94)90017-5

Reading H G, Richards M. 1994. Turbidite systems in deep-water basin margins classified by grain size and feeder system. AAPG Bulletin, 78(5): 792–822

Shanmugam G. 2016. Submarine fans: a critical retrospective (1950–2015). Journal of Palaeogeography, 5(2): 110–184, doi: 10.1016/j.jop.2015.08.011

Shanmugam G. 2022. 150 Years (1872–2022) of research on deep-wa-

ter processes, deposits, settings, triggers, and deformation: a difficult domain of progress, dichotomy, diversion, omission, and groupthink. Journal of Palaeogeography, 11(4): 469–564, doi: 10.1016/j.jop.2022.08.004

Shanmugam G, Lehtonen L R, Straume T, et al. 1994. Slump and debris-flow dominated upper slope facies in the Cretaceous of the Norwegian and Northern North Seas (61–67°N): implications for sand distribution. AAPG Bulletin, 78(6): 910–937

Shao Lei, Li Xuejie, Geng Jianhua, et al. 2007. Deep water bottom current deposition in the northern South China Sea. Science in China Series D: Earth Sciences, 50(7): 1060–1066, doi: 10.1007/s11430-007-0015-y

Su Ming, Hsiung K H, Zhang Cuimei, et al. 2015. The linkage between longitudinal sediment routing systems and basin types in the northern South China Sea in perspective of source-to-sink. Journal of Asian Earth Sciences, 111: 1–13, doi: 10.1016/j.jseaes.2015.05.011

Sun Rui, Yao Xingzong, Wang Xiayang, et al. 2022. Source-to-sink system and sedimentary characteristics of the lower Miocene submarine fans in the eastern deepwater area of the Qiongdongnan Basin, northern South China Sea. Frontiers in Earth Science, 10: 956594, doi: 10.3389/feart.2022.956594

Suter J R, Berryhill H L Jr. 1985. Late Quaternary shelf-margin deltas, northwest Gulf of Mexico. AAPG Bulletin, 69(1): 77–91

Tan Mingxuan, Zhu Xiaomin, Zhang Zili, et al. 2020. Summary of sedimentological issues and fundamental approaches in terms of ancient "Source-to-Sink" systems. Oil & Gas Geology (in Chinese), 41(5): 1107–1118

Torrado L, Mann P, Bhattacharya J. 2014. Application of seismic attributes and spectral decomposition for reservoir characterization of a complex fluvial system: case study of the Carbonera Formation, Llanos foreland basin, Colombia. Geophysics, 79(5): B221–B230, doi: 10.1190/geo2013-0429.1

Vail P R, Mitchum R M Jr, Thompson III S. 1977. Seismic stratigraphy and global changes of sea level: part 3. relative changes of sea level from coastal onlap. In: Payton C E, ed. Seismic Stratigraphy — Applications to Hydrocarbon Exploration. AAPG Memoir, 1859–1866

Wang Xingxing, Kneller B, Sun Qiliang. 2023. Sediment waves control origins of submarine canyons. Geology, 51(3): 310–314, doi: 10.1130/G50642.1

Wang Xue, Lü Baofeng, Cai Zhourong, et al. 2014a. Comprehensive confirmation of Cenozoic tectonic events in northern South China Sea and their significance on petroleum accumulation. Acta Geologica Sinica (English Edition), 88(S2): 1672–1674

Wang Yeyong, Xu Guoqiang, Pang Xiong, et al. 2019. A method for restoring sedimentary sequence original structural profiles: a case study of Miocene strata from the northern continental slope of the South China Sea. Marine and Petroleum Geology, 103: 294–305, doi: 10.1016/j.marpetgeo.2019.01.036

Wang Shangxu, Yuan Sanyi, Yan Binpeng, et al. 2016. Directional complex-valued coherence attributes for discontinuous edge detection. Journal of Applied Geophysics, 129: 1–7, doi: 10.1016/j.jappgeo.2016.03.016

Wang Yahui, Zhang Daojun, Chen Yang, et al. 2014b. Characteristics and controlling factors of Meishan deep-water fans in Lingshui Sag, Qiongdongnan Basin. Xinjiang Petroleum Geology (in Chinese), 35(6): 664–667

Weimer P, Rowan M G, McBride B C, et al. 1998. Evaluating the petroleum systems of the northern deep Gulf of Mexico through integrated basin analysis: an overview. AAPG Bulletin, 82(5B): 865–877

Xia Shiqiang, Liu Jingyan, Liu Zhen, et al. 2018. The geophysical identification, characteristics, and petroliferous significance of sublacustrine fan deposits in the second member of Dongying Formation in Liaozhong Depression, Bohai Bay Basin. Geological Journal, 53(2): 692–706, doi: 10.1002/gj.2921

Xu Guoqiang, Haq B U. 2022. Seismic facies analysis: past, present and future. Earth-Science Reviews, 224: 103876, doi: 10.1016/j.earscirev.2021.103876

Zachos J C, Dickens G R, Zeebe R E. 2008. An early Cenozoic perspective on greenhouse warming and carbon-cycle dynamics. Nature, 451(7176): 279–283, doi: 10.1038/nature06588

Zhang Guilin. 2019. Characteristics of sea level change in the South China Sea since 18.5Ma (in Chinese)[dissertation]. Chengdu: Chengdu University of Technology

Zhang Gongcheng, Feng Congjun, Yao Xingzong, et al. 2021. Petroleum geology in deepwater settings in a passive continental margin of a marginal sea: a case study from the South China Sea. Acta Geologica Sinica (English Edition), 95(1): 1–20, doi: 10.1111/1755-6724.14621

Zhang Yingzhao, Gan Jun, Yang Xibing, et al. 2017. Tectonic evolution and its constraints on the formation of deepwater giant gas field in Lingshui Sag, Qiongdongnan Basin. Marine Geology Frontiers (in Chinese), 33(10): 22–31

Zhang Gongcheng, Qu Hongjun, Zhang Fenglian, et al. 2019. Major new discoveries of oil and gas in global deepwaters and enlightenment. Acta Petrolei Sinica (in Chinese), 40(1): 1–34,55, doi: 10.1038/s41401-018-0042-6

Zhang Gongcheng, Zeng Qingbo, Su Long, et al. 2016. Accumulation mechanism of LS 17–2 deep water giant gas field in Qiongdongnan Basin. Acta Petrolei Sinica (in Chinese), 37(S1): 34–46

Zhao Zhongxian, Sun Zhen, Sun Longtao, et al. 2018. Cenozoic tectonic subsidence in the Qiongdongnan basin, northern South China Sea. Basin Research, 30(S1): 269–288, doi: 10.1111/bre.12220

Zhao Wei, Zhou Chun, Tian Jiwei, et al. 2014. Deep water circulation in the Luzon Strait. Journal of Geophysical Research: Oceans, 119(2): 790–804, doi: 10.1002/2013JC009587

Zheng Hongbo, Yan Pin. 2012. Deep-water bottom current research in the northern South China Sea. Marine Georesources & Geotechnology, 30(2): 122–129

Zheng Hongbo, Yan Pin, Xing Yuqing, et al. 2012. Deep-water bottom current research in the northern South China Sea using a reflection seismic method. Haiyang Xuebao (in Chinese), 34(2): 192–198

Zhu Xiaomin. 2008. Sedimentary Petrology (in Chinese). 4th ed. Beijing: Petroleum Industry Press, 372–378

Zhu Weilin, Huang Baojia, Mi Lijun, et al. 2009. Geochemistry, origin, and deep-water exploration potential of natural gases in the Pearl River Mouth and Qiongdongnan basins, South China Sea. AAPG Bulletin, 93(6): 741–761, doi: 10.1306/02170908099